Emerging Metal-Halide Perovskite Materials for Enhanced Solar Cells and Light-Emitting Applications

Felipe Moreira Pinto, Mary Carmen Mate Durek de Conti, Swayandipta Dey, Esteban Velilla, Carlton A. Taft, and Felipe de Almeida La Porta

1 Introduction

Since the photovoltaic effect was observed for the first time, in particular, many multifunctional materials have widely been developed to facilitate the direct conversion of solar radiation into electricity; thus, enabling the emergence of a promising technology to circumvent the problem of the energy crisis [1–8]. This nearly 70-year-old

F. M. Pinto
Engineering Department, Federal University of Lavras, Lavras, Brazil

M. C. M. D. de Conti · F. de Almeida La Porta (✉)
State University of Londrina, Rodovia Celso Garcia Cid, 445, km 380, Londrina, Paraná 86057-970, Brazil
e-mail: felipelaporta@utfpr.edu.br

M. C. M. D. de Conti
Federal Technological University of Paraná, Nature Sciences Academic, Avenida Alberto Carazzai, 1640 CEP, Cornélio Procópio, PR 86300-000, Brazil

S. Dey
Department of Applied Physics, Institute for Complex Molecular Systems (ICMS), Eindhoven University of Technology, Postbus 513, 5600 MB Eindhoven, The Netherlands

E. Velilla
Centro de Investigación, Innovación y Desarrollo de Materiales—CIDEMAT, Universidad de Antioquia, Medellín, Colombia

C. A. Taft
Centro Brasileiro de Pesquisas Físicas, CBPF, Rio de Janeiro, Brazil

F. de Almeida La Porta
Laboratory of Nanotechnology and Computational Chemistry, Federal Technological University of Paraná, Londrina, Brazil

E. Velilla
Grupo en Manejo Eficiente de la Energía – GIMEL, Universidad de Antioquia, Medellín, Colombia

C. A. Taft and S. R. de Lazaro (eds.), *Research Topics in Bioactivity, Environment and Energy*, Engineering Materials, https://doi.org/10.1007/978-3-031-07622-0_2

technology has quickly developed, branching out into different approaches, almost all of which are based on the operating principle of solar cells. In sum, the basic principles related to the working mechanism of solar cells have been a long study and, in turn, are well established in the literature [1]. Wafer-based silicon solar cells have widely been dominant in this field. Yet, it is well-known that such photovoltaic panels, based on single-crystal silicon, are extremely difficult to manufacture and, in addition, have a relatively high cost [2–4]. Also, as we know, the presence of complex defects on silicon-based solar cells significantly reduction in their photovoltaic performance [5, 7–9].

Hence, especially as a result of high energy demand and consumption, it is fundamentally important to develop alternatives for wafer-based single-crystal silicon that can be cheaper and more efficient. In the middle of the challenges for the use of solar energy on a large scale, metal-halide perovskite materials are emerging as promising alternatives to single-crystal silicon [10–15]. Particularly, such emerging materials have a versatile, easily obtainable structure that is, in turn, tolerant to "defects", but even so, unlike what happens in silicon, electrons manage to permeate these imperfections [16–21]. Consequently, a wide variety of strategies have widely been developed to design single-junction metal-halide perovskite solar cells architectures at a low-cost. Thus, within a decade, the single-junction metal-halide perovskite solar cells had a spectacular increase of their power conversion efficiency (PCE) from 3.8 to 25.7%, that is, making this promising technology to large-scale commercialization [22, 23] as shown in Fig. 1a. Despite this remarkable and impressive progress towards marketing of metal-halide perovskite-based technologies in the future, it should be noted that these PEC results usually are obtained more precisely for the small perovskite-based solar modules (i.e., with area up to 0.1 cm^2) [23–31]. However, it is essential to highlight that perovskite-based solar module area scaling-up has a significant PEC decrease (see inset in Fig. 1a). Thus, the quality of the metal-halide perovskite layer is widely recognized as the key to obtaining high PEC values. Therefore, from this perspective, it should note that the fabrication of metal-halide perovskite films quality in large-area is still a challenge to future commercializing of this technology [23–31].

In terms of devices, many directions were systematically investigated, and from this perspective, four well-established architectures stand out [32–34] Fig. 1b illustrated the architecture standard planar and mesoporous (n–i–p) devices as well as inverted planar and mesoporous (p–i–n) devices. In addition to these architectures, in particular, there is also the mesoscopic structure that is based on the stacking of a mesoporous TiO_2 layer, ZrO_2 spacer layer, and a carbon electrode and does not require an additional hole transporting layer (HTL) [32, 33, 35, 36]. However, it is important to emphasize that this mesoscopic architecture will not be discussed in this chapter.

Also, it is well-known that the best PEC results related to photovoltaic performance are for perovskite-based solar cells containing lead. In general, there is great concern about the toxicity of compounds based on lead, due to their high levels of bioaccumulation as well as a high reactivity [37–42]. These metal, for example, do not exist naturally in any living organism; do not perform nutritional or biochemical

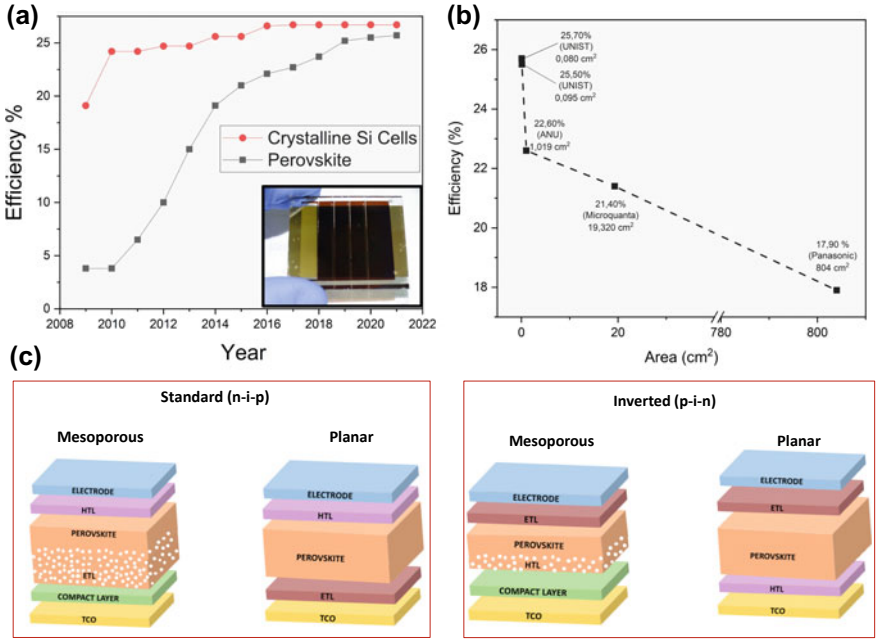

Fig. 1 **a** Comparative representation of the progress in recent years on the PEC efficiency for silicon- and perovskite-based solar cell technologies (adapted from Refs. [28, 29]). The digital picture inset in (**a**) shows a perovskite-based solar cell device manufactured in our laboratory. **b** Measures compared without distinction between eligible cell areas: total area, opening area and designated lighting area (adapted from Refs. [28, 29]). **c** Schematic representation of the four main types of metal-halide perovskite solar cells architectures (adapted from Ref. [31])

functions, so the presence of these metals is highly harmful in any concentration [43]. Therefore, from this perspective, mainly due to the high toxicity of lead, there are currently several studies aimed at replacing this element with other metallic ions, such as Sn^{2+}, Ge^{2+}, Cu^{+}, Ag^{+}, Bi^{3+}, Sb^{3+}, In^{3+} and so on [44–50]. Until now, these emerging metal-halide perovskite-based devices are still suffering from film instability, which usually leads to reduced lifetime of these devices. Further, mainly owing to their myriad outstanding properties, it is notable that these emerging metal-halide perovskite materials to be promising candidates for next-generation of light emitters.

Hence, this chapter compiled the current progress in understanding the structure-composition-property relationship of light emitters and solar cells devices based on emerging metal-halide perovskite materials. Here, a particular emphasis has been put on the structure design and advanced characterization of these emerging metal-halide perovskites prepared by spin coating as a strategy.

2 Emerging Metal-Halide Perovskite Structures

From a geochemical point of view, it is well known that the name perovskite is due to the mineral $CaTiO_3$ (calcium titanate), which was the first example of this family of discovered materials in 1839 by the mineralogist Gustavus Rose [51]. Thus, this fascinating class of perovskite materials (all-inorganic or hybrid) has the general formula ABX_3, where A and B are cations and X are anions (most often O^{2-} or halide ions F^-, Cl^-, Br^- and I^-), although perovskites with nitrides (N^{3-}) and hydrides (H^-) can also be synthesized [51–66].

Among these advanced multi-functional materials, in particular, the inorganic or hybrid metal-halide perovskites, based on the general stoichiometry ABX_3 (e.g., $CsPbX_3$ with X being Cl, Br, I or a mixture thereof), have myriad properties that are key to use in diverse optoelectronic technologies [22, 42, 67–73]. As is well-known, the charge balance of a perovskite-like structure usually is obtained through the sum of the formal oxidation states of the two metals, which occupy the A and B sites, and of the anion, which must total zero (neutral charge). For instance, in oxide perovskites, it is well-known that the sum of the oxidation states for the two cations must be six, so $A^{I}B^{V}O_3$, $A^{II}B^{IV}O_3$ and $A^{III}B^{III}O_3$. On the other hand, more specifically in the case of the metal-halide perovskites, the sum of the oxidation states for these two cations must be three, so the only possible ternary combination is $A^{I}B^{II}X_3$ [74]. Also, it is well-known that these multi-functional materials can easily be obtained in high complexity structures (such as 3D, 2D, 1D, and 0D) by a wide variety of synthetic strategies [53].

As we know, the ideal metal-halide perovskite has a cubic structure belonging to $Pm\bar{3}m$ space group [75, 76]. Until now, most studies have focused on this specific structure; however, it is well-known that depending on the tilting/rotation of the $[BX_6]$ polyhedral clusters in the ABX_3 lattice, particularly this material can also adopt other phases: such as β-tetragonal and two γ- and δ-orthorhombic, respectively, in addition to the desired α-cubic structure [53, 62, 74, 77–85]. Hence, in this perspective, Goldschmidt [86] has introduced an empirical factor, usually known as the Goldschmidt tolerance factor (τ), which is a well-established dimensionless indicator for predicting stability of the cubic perovskite-like structure, which can be defined by the ratios of the ionic radii constituting A, B, and X (Eq. 1). That is:

$$\tau = \frac{\mathrm{Ra} + \mathrm{Rx}}{\sqrt{2}(Ra + Rb)} \tag{1}$$

Hence, based on this empirical factor the cubic structure is most stable in the range of $0.8 < \tau < 1.0$ [86]. When the ratio of the ionic radii deviates from the ideal value range, particularly geometric deformations and distortions of the crystal arise, leading to the stabilization of other phases described above [87]. For instance, Li et al. [88] studied 186 complex ABX_3 systems based on metal-halide perovskites by the Goldschmidt tolerance factor, where they obtained an accuracy of about 96% in predicting the stability of the cubic phase. In the last 95 years, the stability of cubic

metal-halide perovskites has been usually evaluated by using this empirical factor; however, it is well-known that its accuracy is often insufficient [89]. In this regard, several modifications were developed to improve the accuracy of these predictions to accelerate the development process of these materials. Zhang et al. [87] investigated a series of 376 ABO_3-like compounds in order to establish a new criterion to determine the structural stability of perovskite-like compounds. For this, these authors relied on the bond lengths of crystal lattice former (A—O) and crystal lattice modifier (B—O) derived from the bond valence model for the calculations of the tolerance factors, which are found in the range of 0.822–1.139. Therefore, the overall instability for the compounds was identified as being less than 1.2 vu (valence units) as well as increases with decreasing oxidation state of B cations (i.e., $A^{+}B^{5+}O_3$-type > $A^{2+}B^{4+}O_3$-type > $A^{3+}B^{3+}O_3$) [87]. In addition, Bartel et al. [89] have also proposed a new tolerance factor, which is more accurate that the Goldschmidt tolerance factor, defined in the following equation (Eq. 2). That is:

$$\tau = \frac{r_X}{r_B} - n_A\left(n_A - \frac{rA/rB}{ln(rA/rB)}\right) \tag{2}$$

where n_A is the valence of cation A, and r_A and r_B are specifically the values of ionic radii of the cations A and B (being $r_A > r_B$ by definition). According to this new tolerance factor, both oxidic and halide perovskite assume a stable cubic structure when $\tau < 4.18$ [89]. Also, as mentioned before, mainly due to the high toxicity of lead-based compounds, however, there are currently several studies aimed at replacing this element with other metallic ions, as well as, including the present mixed species in the B site [47–50, 90]. These strategies involving different combinations have been extensively investigated in this field to identify new lead-free halide perovskites (see Fig. 2b) that are potentially promising for applications in solar cells and as light emitters.

In addition to the formal ABX_3 stoichiometry, it is possible to obtain perovskite-like materials ordered by vacancy (e.g., A_2BX_6 and A_3BX_9) where the sites of cations A and B are partially or totally vacant, or replaced by a combination of other cations [91–94]. As we know, double perovskite-like structures, converted into a quaternary formula $A^{I}{}_2B^{I}B^{III}X_6$ are usually formed by a mixture of monovalent (B^{I}) and trivalent (B^{III}) cations coexisting together in the crystal lattice [92–94]. The main strategies used to replace Pb in perovskite-type materials: (i) using homovalent elements (e.g., Sn, Ge, and the other) (ii) based on the use of heterovalent elements (e.g., Bi and Sb) that are usually divided into two subcategories: ion splitting and vacancy-ordered formation [94]. Hence, from this perspective, we believe that a more fundamental understanding of these structural alterations is, of course, the key to the future commercialization of optoelectronic technologies based on inorganic or hybrid halide perovskites.

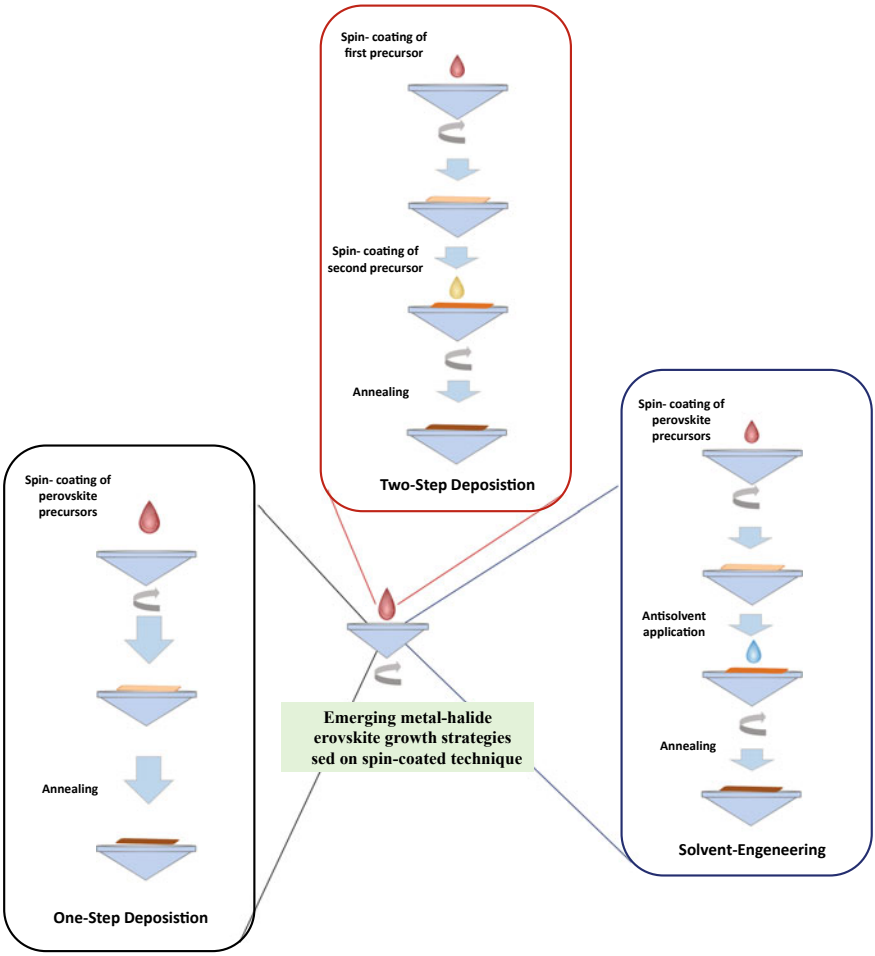

Fig. 2 Diagram showing the most used techniques for the formation of emerging metal-halide perovskite layers (adapted from Ref. [144])

2.1 Homovalent Elements

To replace lead in the all-inorganic and hybrid halide perovskite structure, the easiest is to replace with cations of similarly ionic radii and in the (+2) oxidation state. Thus, in this direction, the most obvious choice would be to replace Pb^{2+} with another atom from Group IV in $AB(II)X_3$ lattice. In particular, an interesting alternative is the replacement of this element by tin, since Sn^{2+} has a very similar ionic radius to Pb^{2+}, 1.35 Å and 1.49 Å, respectively. All-inorganic and hybrid Sn-halide perovskites showed promising optoelectronic properties, as well as, have an attractive bandgap value in the range of 1.2–1.6 eV [95, 96]. In addition, the researchers

have observed for these Sn-based perovskite materials a long diffusion length and electronic mobility than superior to traditional semiconductor materials, such as CdTe and Si, which have been often used in solar panels [44, 72, 97–102]. However, despite the remarkable properties of this $ASnX_3$ system, where A can be most often methylammonium (MA), formamidinium (FA), and cesium (Cs), these perovskites are highly sensitive to moisture and the presence of oxygen, which cause a rapid process of oxidation from Sn^{2+} to Sn^{4+} and, as a result, the perovskite geometry distorts and the optical and electronic properties change significantly during this process [67, 102–104].

Another candidate for replacing Pb in perovskites is germanium itself, Ge^{2+}, previously mentioned [105–107]. In the Cs-Ge-X ternary system, there is a bandgap value at room temperature of 1.6 eV for $CsGeI_3$, 2.3 eV for $CsGeBr_3$, and about 3.2 eV for $CsGeCl_3$, respectively. Thus, it is observed that the bandgap increases with the decrease of the ionic radius of the halogens (2.20 Å, 1.96 Å, 1.81 Å) [72]. All-inorganic halide perovskites based on germanium exhibit a crystal structure formed by octahedral clusters of $[GeX_6]^{4-}$ similar to that observed in lead halogenate perovskites. Under ambient conditions, in particular, the $CsGeCl_3$ phase has a cubic crystal structure, while the bromine ($CsGeBr_3$) and iodine ($CsGeI_3$) halides have a distorted rhombohedral structure, which is caused by the second-order Jahn-Teller effect [105]. Sun et al. [106] have investigated the $MAGeX_3$ (X = Cl, Br, I) properties through theoretical calculations and observed similarity to the $MAPbI_3$ compound in terms of the conductivity, stability and optical properties.

Nagane et al. [108] synthesized perovskites varying the composition of Sn-Ge and studied their application in solar cells. For Ge-doping $MASnI_3$, a phase-transition of tetragonal-to-trigonal was observed from the $CH_3NH_3Sn_{0.25}Ge_{0.75}I_3$, which increases the tolerance factor from 0.84 (pure $MASnI_3$) to 0.93 ($MASn_{0.25}Ge_{0.75}I_3$), as well as, the stability of such-doped samples [108]. Also, the bandgap of this Sn-Ge based halide perovskites have a bandgap value in the range of 1.3 eV ($MASnI_3$) to 1.9 eV ($MASn_{0.25}Ge_{0.75}I_3$), respectively. In addition, the $MASn_{0.5}Ge_{0.5}I_3$ composition showed a bandgap of 1.5 eV with low structural disorder [72]. However, it is known that Pb^{2+} has a better applicability due to its superior stability when compared to Sn^{2+} and Ge^{2+}.

On the other hand, Filip and Giustino have performed a computational screening of all homovalent metal ions (B-site +2 cations) that could replace lead in a perovskite halide configuration [98]. For this computational study, were adopted two criteria that are important for solar cell applications. Firstly, the stability of the cubic perovskite-like structure. Secondly, a direct bandgap value smaller than 2 eV. In this way, a series investigated of perovskite compounds have a reduction from 248 to 25, based on these two criteria, of which 15 have not yet been proposed for used in solar cells. Finally, these authors concluded that the partial replacement of Pb by Mg can help to reduce the toxicity of hybrid halide perovskite, at the same time maintaining its remarkable optoelectronics features [98]. In addition, Korbel et al. [109] performed an extensive study on perovskite-like materials, from over 32,000 possible ABX_3 combinations, with only 199 hypothetical perovskites being stable (within 25 meV) in nice agreement with study of Filip and Giustino [98].

2.2 Heterovalent Elements

2.2.1 Ion Splitting Subcategory

Firstly, in this subcategory, we will initially address the mixed anionic compounds, with general formula $AB(Ch,X)_3$, where Ch = chalcogen and X = halogen [94, 110, 111]. Such compounds has been recently examined by Sun et al. [112]. These authors found that the $CsSnS_2Cl$ exhibits optical properties most relevant to applications in solar cells than for $CsSnI_3$. In this way, it is well-known that most of the work on $AB(Ch,X)_3$ is based on the Bi (non-toxic heterovalent elements) replacing the Pb element; causing it to maintain the 3D perovskite structure and charge neutrality, and the anion was replaced by dual (halogen and chalcogen) anions. Among these materials, especially $MABiSI_2$ and $MABiSeI_2$ being highlighted, due to their optimal bandgap value (1.3–1.4 eV) for applications as solar cells [100]. Also, it is known that the substitution of Pb by Sb or Bi in $AB(Ch,X)_3$ compounds reduces its dimensionality structural, that is, leading to new and tunable physical properties [113]. As we know, the mixed chalcogenide–halide-based perovskite formation leads to higher stability structural. In turn, it is an exciting feature for lead-free halide perovskites, which still face major stability problems. This fact has been usually assigned to the more covalent bond character found for these compounds [110]. Although none novel absorber materials has been identified from this new class of perovskite-like compounds [97]; however, it is important to emphasize that the research with these chalcogenide-halide-based systems is still in its infancy. Finally, from this perspective, it has been widely recognized that chalcogenide-halide-based systems has latent potential for many optoelectronics applications, and for this reason they promise to shake up this important field of research in the future.

2.2.2 Mixed Cationic Compounds

To make up for the problems related to the replacement of Pb by Sb or Bi elements, the strategy of obtaining double halide perovskites, $A_2B(I)B(III)X_6$ type, with substitution of the B site by mixed cations ($B = B^+$, $B' = B^{3+}$) was explored [114, 115]. Zhao et al. [116] proposed a classification, in terms of electronic structure and chemical stability for the elements that can occupy the BI-site ($A_2B(I)B(III)X_6$). Based on these results, elements of group IA (Na^+, K^+, and Rb^+) contribute to the increase BI-s orbital energy, raising the conduction band position. While that elements of group IB (Cu^+, Ag^+ and Au^+) may provide a significant variation in bandgap value as well as is responsible for changing the valence band of these materials. On the other hand, these authors also identified that use of elements of group IIIA (In^+ and Tl^+) induces an expansion of the octahedron $[B(I)X(VII)_6]$ clusters as well as contribute to a reduction of the octahedron $[B(III)X(VII)_6]$ clusters. Such structural alterations may contribute to raising the top of valence band in $A_2B(I)B(III)X_6$ compounds [116]. Also, in such compounds, it has been observed that increasing the ionic radius of

the halogen contributes to a reduction in the bandgap, while the B(III) site change, e.g., from Sb^{3+} to Bi^{3+}, leads to a significant increase in the bandgap [114]. Finally, the alkali metal cations selected to occupy the B(I)-site not contribute ionicity to the band edges.

$A_2B(I)B(III)X_6$ perovskites are also known as "elpasolites", named after the mineral K_2NaAlF_6. Giustino et al. [39] verified the chemical elements of the periodic table that belong to the elpasolite halides. In their research the authors report 7 elements for the A-site (cations), 8 elements for the B(I)-site (including NH^{3+} and $CH3NH^{3+}$), 34 elements for the B(III)-site (cations) and 5 elements for the X-site (including cyanide CN^{-}) [39].

Double halide perovskites with alkali metal B(I) cations have 0D dimensionality and have a wide-bandgap feature [94, 117–119]. However, for these complex structures, transition metal cations with multiple oxidation states and/or partially occupied d or f orbitals are not desirable for the B(III)-site [94]. Because they can introduce deep defect states and very low band edges located [94]. Finally, the anions of halides to the X-site, as mentioned before, as the halides change from F^{-}, Cl^{-}, Br^{-} to I^{-}, the bandgap generally decreases [116, 120–124]**.**

Furthermore, the vacancy-ordered double perovskite structures, with formula $A_3\square B(III)X_9$ or $A_2\square B(IV)X_6$, has been the focus of several studies and usually are structurally characterized by an antifluorite array of isolated octahedral units linked by A-site cations [125]. These phase transitions in these systems are driven by a mismatch in the ionic radii of the constituent atoms [126].

In the case of the $A_3\square B(III)X_9$ compounds, the replacing Pb(II) with a group 15 element will result in materials that can assume a 2D or 0D crystal structure [127]. Chang et al. studied the crystal structure of the following synthesized compounds $Rb_3Sb_2Br_9$, $Rb_3Sb_2I_9$, $Rb_3Bi_2Br_9$, $Rb_3Bi_2I_9$ and $Tl_3Bi_2Br_9$. The crystals obtained showed two types of double-layered crystal structures, which are characteristic of the sharing of corners of the BX_6 octahedron. The differences between the $A_3B_2X_9$ types can be attributed to specific structural distortions in the close packaging of the underlying AX_3. In this way we have two polymorphisms for the compound $A_3B_2X_9$ [128]. For instance, the $A_3Bi_2X_9$ vacancy-ordered perovskite-like materials can crystallize most commonly in a trigonal structure (P3m1 space group) of low dimensionality. Likewise, in particular, $Cs_3Sb_2I_9$ can crystallize into 0D shape (P63/mmc space group) and the 2D <111> stacked layer shape (P3m1), respectively [114, 129–131]. Pal et al. [132] suggest that colloidal nanocrystals $Cs_3Sb_2I_9$ (nanoplatelets and nanorods) and $Rb_3Sb_2I_9$ have the potential for optoelectronic applications. In addition, Chonamada et al. [133] has been reported the degradation ratio for both polymorphs of $Cs_3Sb_2I_9$ in form of thin film by the effect of light, water, and heat under an ambient atmosphere. Despite the simplicity of being prepared with controlled particle size and morphology, in general, such materials are highly chemically unstable and this represents a major challenge for their use and commercial exploitation.

For $A_2\square B(IV)X_6$ vacancy-ordered perovskite-like materials, containing non-toxic transition metals that have a stable +4 oxidation state are promising materials for photovoltaic application [134]. In this sense, Sakai et al. [135] have reported a

series of $A_2\square B(IV)X_6$ compounds, with A = Cs^+, B = Pd^{4+} and X = Br^-, with cubic crystal structure ($Fm\bar{3}m$ space group) obtained from direct oxidation of Pd^{2+} to Pd^{4+} in solution. Among these systems, the authors identified that Cs_2PdBr_6 has a bandgap of about 1.6 eV and hence is a promising candidate for applications in solar cells and as light emitters [135].

Theoretical and experimental investigations on the Cs_2TiI_6, Rb_2TiI_6, K_2TiI_6 and In_2TiI_6, have revealed excellent physical properties for used of such compounds in optoelectronic technologies [136]. The band structures of these A_2TiI_6 vacancy-ordered perovskite-like materials show a very dispersive conduction.

López-Fraguas et al. [137] analyzed the fast structural evolution due to degradation of the $CsSnI_3$ films leading to the formation of the Cs_2SnI_6. These authors reported that PLQY for these film deceases significantly. In general, it is well-known that the oxidized Sn^{4+} ion in perovskite-like structures can act as a p-type dopant, inducing a process of self-doping, that in turn limits its efficiency in energy conversion [72, 138]. To avoid the Sn^{2+} oxidation process, Lee et al. [107] used the SnF_2 compound as a reducing agent in the formation of $FASnI_3$. While that the Umedov et al. [139] have demonstrated the effect of adaptation of the A site (by the addition of Rb and Ag) on the stability of the Cs_2SnI_6 films in ambient air.

3 Synthesis Protocol for Emerging Metal-Halide Perovskites

One of the greatest advantages of metal-halide perovskite-based solar cell technology, compared to other technologies, is precisely the manufacturing simplicity with tunable properties [140]. Thus, the long path for the evolution and development of metal-halide perovskite-based devices was marked by a constant improvement of deposition techniques, an evolution achieved from an increase in the understanding of crystallization processes [141]. Particularly, it is well-known that the kinetics of the perovskite formation reaction is relatively fast, and there are several film formation methods that confirm this kinetics. Hence, the quality of the metal-halide perovskite films depends on optimizing parameters related to the concentration of precursors, solvent, temperature, rotation speed, time, and even the post-deposition processes [142–144].

In particular, spin-coating is a solution-based strategy for the simple fabrication of thin films at a low cost, which has received a lot of attention amid the metal-halide perovskite preparation methods [144]. For this reason, in this work we will highlight the recent advances made based on the use of this simple strategy. Figure 2 shows the most used perovskite growth strategies based on spin-coated technique [144]. Of course, spin-coating can produce thin films of high quality with controlled and uniform thickness (i.e., if the viscosity is homogeneous over the entire area of the substrate, regardless of the slip force) [145, 146], even in dry-box conditions and substrate up to 100 cm^2 [147, 148]. During the spin of the substrate, the

centripetal force overcomes the gravitational force and the solute is spread throughout the substrate, forming a film. The substrate in constant speed rotation causes uniform evaporation of the solvent, therefore it is expected that the film thickness will also become uniform [149]. Furthermore, it is well known that the volatility of solvents affects the crystallization process of thin films significantly [150]. Finally, as is well known, the film thickness resulting is, in turn, dependent on the solution concentration of the target material used as well as is usually proportional to the inverse of the spin speed squared (in the case of the same concentration) [145, 146, 150].

3.1 One-Step Deposition

In this approach, all precursors of the final material are added in a single solution, which is subsequently deposited under the substrate, followed by a heat treatment step. The main aspect of this deposition strategy consists of mixing organic and inorganic precursors in common solvent(s), generally gamma-butyrolactone (GBL), and/or dimethylsulfoxide (DMSO), and/or, dimethylformamide (DMF) as well as the combination of more than one solvent [151–153]. The physical-chemical differences between the organic and inorganic species imply, among other issues, difficulty in obtaining an adequate dissolution of both precursors in a common solvent, resulting, therefore, in films with flaws and moderate coverage rate [151]. Although this approach is extensively used and simple, the precursors used can undergo several chemical reactions in the mixture, influencing both the resulting film and the performance of photovoltaic devices [154].

3.2 Two-Step Deposition

In this approach, the inorganic and organic compounds are dissolved separately and deposited in sequence (inorganic compound is dissolved in DMSO or DMF and the organic one in Propanol) [143, 155, 156]. The inorganic compound is deposited first, after heat treatment, the organic compound dissolved in propanol is deposited, since inorganic compounds, such as PbI_2 and others, used do not dissolve in propanol. Additional control over the thin film morphology can then be obtained with this deposition strategy, as it is possible to obtain uniform cuboid perovskite crystals, while the one-step method usually presents an irregular morphology as well as have a high density of pinholes [155]. In addition to the possibility of creating layers of different materials, based on deposition in more than one step makes it possible to create surfaces with different characteristics that can bring greater light absorption and consequently induce higher PCEs values for metal-halide perovskite solar cells [157]. Zheng et al. [158] studied a one-step spin-coating process and compared it with two-step spin-coated, in which the best photovoltaic performances of the perovskite devices with a rough interface of perovskite, which was synthesized with two-step

spin coated as strategy. Despite that, the deposition in two steps or even more steps present an equally challenging and expensive, since there is a production step at each new synthesis step, that is, an additional expense from a commercial point of view. Nevertheless, using this approach, it is possible to obtain perovskite in nanoscale size that can be used as a sensitizer in dye-sensitized solar cells [159, 160] expanding the perovskite applicability to other photovoltaic technologies or light-emitting devices [161–166].

3.3 Solvent-Engineering

Among the strategies of film deposition that have brought good results in metal-halide perovskite solar cells is, of course, the solvent engineering protocol [167–170]. Jeon et al. [171] have in addition to using two solvents simultaneously, GBL and DMSO, was the first to report the use of an anti-solvent method, obtaining perovskite films of high crystalline quality, and indeed, high PEC values of about 16.2%. In general, this approach consists of preparing a perovskite solution usually based on a solvent mixture (DMSO/GBL or DMSO/DMF) capable of producing denser layers than the conventional one-step method, taking advantage of the control of the crystallization process [172]. During the last seconds of spin coating rotation, a perovskite non-solvent (e.g., toluene, chlorobenzene, dichlorobenzene or diethyl ether) is placed on the perovskite film, leading to the formation of the $MA_2Pb_3I_8.2DMSO$ intermediate [168–170]. The DMSO molecules do not allow the direct formation of perovskite to occur, thus forming an intermediate, which with heat treatment loses the DMSO molecules, forming perovskite [167]. This deposition strategy, in particular, have achieved PEC values above 20% [173, 174]. Xiao et al. [175] studied the conventional one-step method followed by a subsequent addition of chlorobenzene (CBZ) leading to an acceleration of the formation of the perovskite layer with greater homogeneity, and consequently higher quality. Jeon et al. [173] observed that with the use of the solvent engineering technique (addition of toluene) there is the formation of a dense film and totally covered in TiO_2. In addition to the change for the better in the density and quality of the formed film, there was also an acceleration of the drying process of the perovskite film. Furthermore, it has been observed that solvent engineering strategy lead to a redissolution of the grains and later recrystallization faster, that is, causing the grain size to be close to the film thickness [176]. Although solvent engineering technology is a promising methodology, two important issues remain to be resolved. First, the effect of non-polar solvent on the mechanism of perovskite adduct formation, and second the ratio that leads MAI-PbI_2-DMSO adduct plays a more important role in the crystallization process than MAI-PbI_2-dimethylformamide (DMF) is also unclear [172].

4 Opportunities in Optoelectronic Technologies

4.1 Applications as Light Emitters

With the ever-increasing demand and consumption of various lighting and electronic display devices consuming more than 20% of worldwide electrical energy per year, it is imperative to develop more energy-efficient devices [177–180]. In terms of electroluminescence types, it has been demonstrated that both the narrowband emission derived from free excitons as well as broadband white light emission arising from self-trapped excitons could prove to be quite beneficial in light-emitting applications [179, 181, 182].

As is well-known, the nature of the optoelectronic behavior on semiconducting materials relies on the efficiency of carrier separation between the photogenerated charge carriers and the subsequent carrier recombination for mutual conversion between light and electricity [138, 183–185]. Due to their unique optoelectronic properties such as superior light absorption, excellent carrier transport performance arising from long diffusion lengths, high photoluminescence quantum yields (PLQY), low exciton binding energies, along with their strong defect tolerant behavior make this class of emerging multi-functional materials such potential candidates for developing next generation optoelectronic devices [15, 53, 127, 185–191]. Despite having such fascinating optoelectronic properties, the widescale commercialization process of emerging metal-halide perovskite materials hasn't been kicked off due to intrinsic material toxicity and inferior stability to silicon-based technologies [15, 33, 192]. Therefore, it is imperative to address the existing challenges alongside a continuous search of emerging metal-halide perovskite-based semiconductors, especially lead-free compounds, with improved optoelectronic performance that will hold the key to the future development these field [185, 193–195].

In principle, usually, an excellent light-harvesting material should also be good light-emitting material, but the materials used and the design principles require different approaches whether the materials are applicable in photovoltaic or light-emitting devices [52, 196, 197]. For light-emitting devices, it is well-known that the efficient and fast radiative recombination of excitons is quintessential, whereas, for photovoltaic devices like solar cells, effective charge separation of excitons is critical to extract the charges and convert the charges light to electrical power generation [198–203]. As such, the family of metal-halide perovskites offers a rich variety of convenient frameworks to systematically study the effects of dimensionality, composition, and structural disorder on its electronic configuration and how it affects the optoelectronic properties of the materials [15].

In metal-halide perovskites, within a given dimensionality, the optical response is readily modified through substitution of the halide component leading to alteration in the valence band positions [73, 204, 205]. Generally, in mixed-halide-based perovskites, such as $CsPb(Br_{1-x}Cl_x)_3$ or $CsPb(I_{1-x}Br_x)_3$, it provides emission tunability in the range from 400 to 700 nm with PLQY varying anywhere from 50 to 90%. Whereas, in a mixed cations-based systems, such as $(FA_{1-x}Cs_x)PbI_3$, it offers

less optical tunability with bandgaps residing in the range of 1.48– 1.73 eV [73, 204, 205]. This bandgap variation in mixed cations-based halide perovskites is primarily due to modified spin-orbit coupling at the edge of the conduction band. Significant changes in the optical properties have been observed upon dimensionality reduction, particularly in the quantum confined two-dimensional layered Ruddlesden-Popper like perovskite analogs (quantum wells). Such complex structures possess enhanced exciton binding energies (reduced PL lifetime) leading to giant oscillator strengths and optical non-linearities [206–210]. Stokes-shifted PL bands also arise from bound exciton states depending on the organic component resulting in modification of dielectric environment [206–208, 211, 212]. Besides being temperature-independent, the strong exciton-phonon coupling has also been reported for some 2D perovskites $(C_6H_5C_2H_4NH_3)_2PbI_4$, which directly attributes to polaron formation. On the other hand, self-trapped excitons (and biexcitons) in atomically thin, layered 2D perovskites sheet-like structures display a significant role in the non-linear optical response, mainly due to the enhanced binding energy. Hence, it is well-known that the optical response of 2D perovskite-based LEDs can, in principle, be easily modulated by rational varying the organic cations, organic chain, layer number, and so on. The performed initial reports on physical properties of pure phase 2D perovskite-based LEDs has been realized for $(CH_3(CH_2)_3NH_3)_2(CH_3NH_3)_{n-1}Pb_nI_{3n+1}$ Ruddlesden-Popper like systems [206–208]. These vertically oriented films were conducive to efficient charge injection and transport, leading to high electroluminescence efficiency. Due to the phase purity of 2D perovskites, it is expected that LEDs will demonstrate high stability, being operational at low turn-on voltages and could be driven at a high current density of a few A/cm^2. Later in 2017, Chen et al. [213] introduced aromatic alkyl amines into 2D perovskites, which changed the crystal structure from cubic to rod-like and finally a thin film. Interestingly, the electroluminescence of the resultant LEDs was tunable from green to blue just by modifying the structure. Besides modification of materials, altering the device processing and fabrication could also play an important role. For example, in 2018, Yang et al. [214] used a quasi-2D perovskite through composition and phase engineering, thereby obtaining thin films with efficient external PLQY reaching up to 14.36%. In addition, the crystallization process could play a key role affecting the optoelectronic properties of the material. Based on this, Quan et al. [215] explored how different bandgap domains affect the PLQY and LED performance by preparing 2D perovskite-based on $PEA_2(MA)_{n-1}Pb_nBr_{3n+1}$ and engineered solvent composition during the crystallization process, thereby achieving a EQE of 7.4% with an average brightness of the fabricated LEDs close to 8400 cd/m^2.

Lead-free double perovskite variant based on $Cs_2AgInCl_6$ with low dimensionality has been recently proposed as warm white-light emitters exhibiting a broadband spectrum in the range of 400–800 nm [216, 217]. From stability point of view, all-inorganic perovskite variants exhibit higher stability than organic-inorganic counterparts. In contrast, the 2D or layered organic-inorganic perovskite variants show higher stability against moisture than their 3D all-inorganic counterparts. Some studies also noted that $A_3B(III)_2X_9$ QDs exhibit wider PL spectra and larger Stokes shift compared to 3D $MAPbX_3$ QDs which could be attributed to strong electron-phonon

coupling [218–220]. On the other hand, $Cs_3Cu_2I_5$ represented an all-inorganic 0D lead-free perovskite variant exhibiting an efficient broadband blue emission with PLQY reaching up to 90% [221].

Ma et al. [222] investigated $Cs_3Sb_2X_9$ 0D particles for application in LED devices, specifically in the 385–640 nm spectral tuning region. Such materials have a high PLQY of about 51.2% and chemical stability. However, it is well-known that the Sb-based halide perovskites are more prone to deep defects when compared to Pb-based halide perovskites. Recently, Hang et al. [223] have reported the relationship between the PLQY and the particle size of $Cs_2AgBi_{1-x}In_xCl_6$ ($0 < x < 1$). Among these materials obtained, the $Cs_2AgBi_{0.125}In_{0.875}Cl_6$ stands out because it can break the transition prohibited by parity and retain a direct bandgap, emitting warm white light, with a PLQY of about 70.3%. An interesting feature of these results is the light stability exceeding three months (ca. 2160 h) higher than the study conducted by Luo et al. [217] where the value obtained was 1000 h.

For Sn(II)-based variants, Zhou et al. [224] first reported $(C_4N_2H_{14}Br)_4SnBr_6$ with a near unity PLQY, when embedded within an organic matrix in a host-guest fashion, it exhibited a white-light emission with a blue phosphor matrix with a CIE coordinates of (0.35,0.39) and a CCT of 4946 K. Following this work, other two-dimensional Sn-based perovskite variants has been also recently developed with a PLQY of 88% with emission wavelength at 625 nm [225]. Some recent results on the performance of light-emitting devices based on lead-free perovskites are summarized in Table 1. Although these initial few studies are promising, there is still effort required to address a few challenges:

1. The Pb-free perovskite variant LEDs are still far from being commercialized.
2. The PLQY is still a major hindrance as majority of these Pb-free perovskite variants can hardly exceed 80%.
3. The charge generation and recombination, electroluminescence mechanisms are still widely lacking, thus rational design principles (especially with the charge transport layers) has not been well established yet wherein can freely control emission spectra.

Table 1 Representative results related to electroluminescence peak emission (EL), maximum external quantum efficiency (EQE) and maximum current efficiency (CE_{MAX}) for lead-free perovskite-based light-emitting devices

Device architecture	EL λ (nm)	EQE (%)	CE_{max} (cd/A)	References
ITO/PEDOT/$CsSnI_3$/PBD/LiF/Al	950	3.8	n/a	[226]
ITO/PEDOT:PSS/$MASn(Br_{0.2}I_{0.8})_3$/F8/Ca/Ag	868	0.058	n/a	[227]
ITO/PEDOT:PSS/PEA_2SnI_4/TPBi/LiF/Al	633	0.3	n/a	[228]
ITO/PVK/$(PEAI)_{3.5}(CsI)_5(SnI_2)_{4.5}$/TmPyPB/LiF/Al	920	3.0	n/a	[229]
ITO/PEDOT:PSS/Poly-TPD/$CsCu_2I_3$/TPBi/LiF/Al	550	0.17	0.46	[230]
ITO/NiO/ $Cs_3Cu_2I_5$/TPBi/LiF/Al	445	1.12	n/a	[231]
ITO/ZnO:PEI/ $Cs_3Sb_2Br_9$/TCTA/MoO_3/Al	408	0.206	n/a	[232]

Research efforts on exploiting the nanocrystalline nature of inorganic and hybrid halide perovskite-based materials for potential light-emitting applications have only been a few years, with lead-free perovskite, even at very early stages. Although there has been a huge boost in the synthesis and solution processing stages utilizing these materials over the last few years, however, must achieve a further understanding of their optical properties by introducing synergistic experimental and theoretical efforts in the development process. These will give more guidance in establishing the structure-property relationships in terms of the material's electronic property and its stability against heat, light, oxygen, humidity, and so on. These joint efforts may open new doors for next-generation advanced lead-free perovskite-based optoelectronics.

4.2 Applications as Solar Cells

For perovskite-based solar cells, effective charge separation of excitons is critical to extract the charges and convert the charges light to electrical power generation. Therefore, the efficiency of these devices is conventionally defined as the ratio of the output power to the incident power from the light source, per unit area [1]. This efficiency is traditionally measured at Standard Test Conditions (1 sun of light and device temperature of about 25 °C) and reported by manufacturers in order to compare the performance of one device to another regardless of the solar cells technology [49, 99, 127, 233–258].

In the case of perovskite technology, a broad range of efficiencies have been reported because different elements such as architectures (see Fig. 1c), structures, compositions, and layers to extract the charges have been used to fabricate perovskite solar cells. Therefore, the combination of these elements is reflected not only on the efficiency, but also on the stability of devices, opening a lot of roadmaps to improve, for instance, the efficiency or another parameter according to the application [34, 49, 99, 127, 145, 233–258]. In this regard, it is noted that the protocols to fabricate efficient and reproducible devices display a critical role in the development of this technology [34]. Besides, despite that the precursor-solution chemistry can be considered as the key obtaining high-quality films, the coating procedure and perovskite composition must be optimized simultaneously for achieving higher efficiencies considering the particularities of each architecture (n-i-p, p-i-n or mesoporous) [145]. Figure 3 illustrated the energy-band-alignment diagram of some materials available for fabrication of the single-junction metal-halide perovskite solar cells. In general, it is well-known that the nuanced structural differences among interfaces of the target perovskite-based devices are critical to its high-performance applications.

On the other hand, it is worth noted that large-scale manufacturing conventionally involved environmental conditions, thus, the protocols and coating procedures to fabricate perovskite devices must be optimized considering the environmental

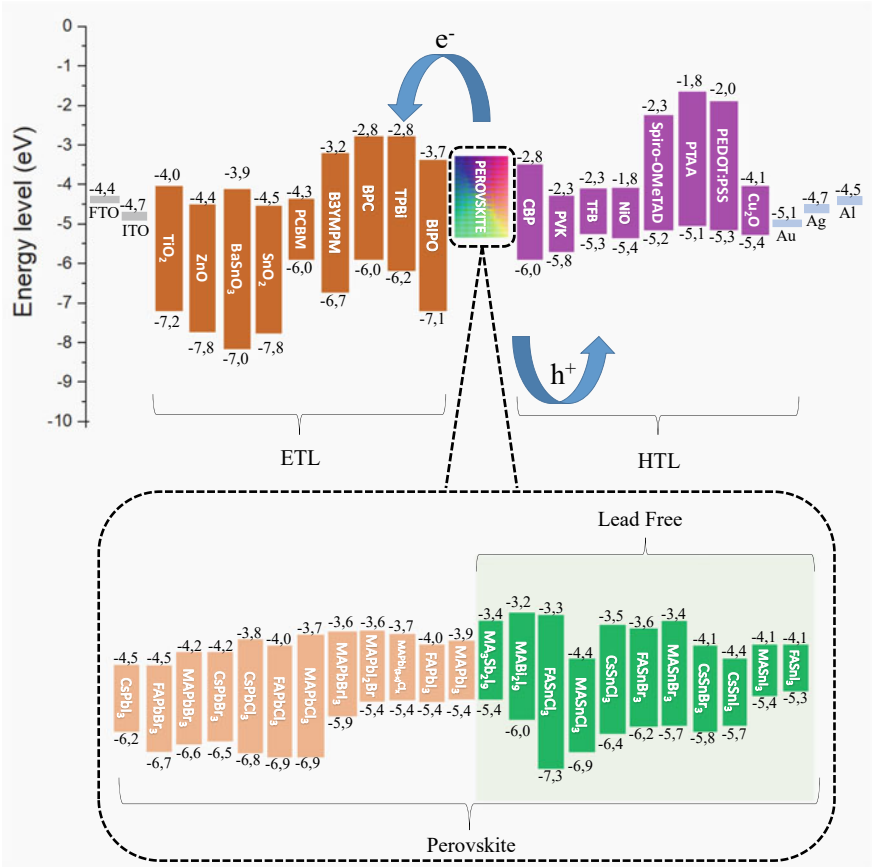

Fig. 3 Schematic energy-band-alignment diagram of emerging metal-halide perovskite-based solar cells based on different materials usually used as electron-transporting layers (ETL) and as hole-transporting layers (HTL)

factors. Moreover, the environmental impact of perovskite processing is predominantly addressed to use the most environmentally friendly solvent for the fabrication process, and the most environmentally friendly elements to mitigate the main drawback related to the toxicity of conventional perovskites [259–273].

Accordingly, Chen et al. [107] have reported the application of Cs_2SnGeI_6-based solar cells. The performance of these devices showed high stability, with less than 10% deterioration in efficiency after 500 h of continuous operation in N_2 atmosphere under sunlight. Park et al. [235] manufactured a solar cell with $Cs_3Bi_2I_9$ perovskite which showed a PEC above 1%. While that the Correa-Baena et al. [260] studied the potential use of $A_3Sb_2I_9$ (A = Cs, Rb and K) compounds, as photoabsorbent in solar cell applications. $Cs_3Sb_2I_9$ has a 0D structure, the highest exciton binding energy (175 ± 9 meV), an indirect bandgap, and low photocurrent in a solar cell (0.13 mA cm^{-2}).

$Rb_3Sb_2I_9$ has a 2D structure, a direct bandgap, and among the materials investigated, the lowest exciton binding energy (101 ± 6 MeV) and the highest photocurrent (1.67 mA cm^{-2}). $K_3Sb_2I_9$ has a 2D structure, intermediate exciton binding energies (129 ± 9 MeV) and intermediate photocurrents (0.41 mA cm^{-2}). Despite remarkably long lifetimes in all compounds (54.9 and 30 ns for Cs, Rb, and K-based materials, respectively), the combination of high exciton binding energy and large effective masses for electrons and holes, results in photocurrents well below 1 mA cm^{-2} which limit device performance [260]. Nie et al. [261] have reported $MASbSI_2$-based solar cell devices, which showed PEC of about 3.08%, under standard lighting conditions of 100 mW/cm^2. Cortecchia et al. [263] have reported 2D $MA_2CuCl_xBr_{4-x}$ based solar cell devices exibiht a low J_{SC} of 216 μA cm^{-2} and V_{oc} of 0.256 V, with a PCE of 0.017%. Abulikemu et al. [264] have reported millimeter-scale $(CH_3NH_3)_3Bi_2I_9$ based solar cell devices with a PCE of about 0.11%, J_{SC} of 491.89 μA cm^{-2} and a V_{oc} of 0.7216 V. Ran et al. [256] synthesized a compact thin film of $(CH_3NH_3)_3Bi_2I_9$ with a PCE of 0.39% and V_{oc} of 0.83 V. These synthesized devices showed low potential loss, but still, a small hysteresis J-V. However, despite these results, the Bi-based perovskite devices have a more stability when compared to Pb-based perovskite devices [256, 264]. Bein et al. [265] manufactured a solar cell with $Cs_2AgBiBr_6$ perovskite which showed a PEC of 2.43%, a V_{oc} greater than 1 V and good stability at ambient conditions, but with a of relevant hysteresis. In subsequent works, performed by Wu et al. [266] and later Li et al. [267], based on using of solvent engineering strategy, has been reported a relevant decrease in hysteresis of the $Cs_2AgBiBr_6$-based devices. Representative results on lead-free perovskite-based solar cell devices are summarized in Table 2.

Although the growing number of studies related to lead-free perovskite have been published, the most efficient and stable perovskite solar cells are based on lead [268]. These facts highlight that there is still much work to do in this topic to avoid the use of lead on the fabrication of perovskite devices. Moreover, it is worth noted that every innovative technology tries to advance in terms of stability, efficiency, lower costs, stability and sustainability when compared to established/predominant technology [269–273]. Currently, there are some challenges for the economic advancement and use of emerging metal-halide perovskite-based technologies such as the stability (a), toxicity (b), upscaling (c) reproducibility (d).

(a) Stability:

In addition to high energy absorption and conversion rates, stability and consequent lifetime are essential factors for a viable commercialization of metal-halide perovskite-based solar cell technologies [271, 272, 274]. Currently, the long-term stability or lifetime (T_{80}) of perovskite-based technology on average is only a few months, even for encapsulated devices [275]. This short lifetime is the result of intrinsic and external aspects [276]. Particularly, the intrinsic degradation is mainly related to thermal and light soaking effects. The external degradation is mainly related to moisture ingress into the device. Therefore, various testing protocols have been used to evaluate and report the stability assessment focused mainly on laboratory-scale cells [277–280]. Besides, in

Table 2 Summary of lead-free perovskite-based solar cells performance prepared by spin coating

Architecture	V_{OC} (V)	J_{SC} (mA cm^{-2})	FF (%)	PCE (%)	References
FTO/cp-TiO_2/mp-TiO_2/$(CH_3NH_3)_3Bi_2I_9$/Spiro-OMe TAD/Au	0.88	0.80	49.71	0.34	[233]
FTO/cp-TiO_2/mp-TiO_2/$MASn(I_{0.33}Br_{0.67})_3$/Spiro-MeOTAD/Au	0.58	11.09	49.50	3.20	[234]
FTO/cp-TiO_2/mp-TiO_2/$Cs_3Bi_2I_9$/HTM/Ag	0.85	2.15	60.00	1.09	[235]
FTO/cp-TiO_2/mp-TiO_2/{en} $MASnI_3$/PTAA/Au	0.43	24.28	63.72	6.63	[236]
FTO/cp-TiO_2/mp-TiO_2/$CsSnBr_3$/spiro-MeOTAD /Au	0.41	~9.00	58.00	2.10	[237]
FTO/cp-TiO_2/mp-TiO_2/$CH_3NH_3SnIBr_2$/Spiro-MeOTAD/Au	0.82	12.30	57.00	5.73	[238]
FTO/cp-TiO2/mp-TiO2/SbSI/PCPDTBT /PEDOT:PSS/Au	0.47	12.00	52.00	2.91	[239]
ITO/cp-TiO_2/mp-TiO_2/$MA_3Bi_2I_9$/spiro-MeOTAD/MoO_3/Ag	0.66	0.91	63.63	0.42	[240]
FTO/cp-TiO_2/mp-TiO_2/$Cs_2AgBiBr_6$/PTAA/Au	1.02	1.84	67.00	1.26	[241]
FTO/cpt TiO_2/mp TiO_2/20% SnF_2-$CsSnI_3$/m-MTDATA/Au	0.24	22.70	37.00	2.02	[242]
ITO/TiO_2/$CsSnI_3$/spiro-OMeTAD/Au	0.86	23.21	65.00	12.96	[243]
ITO/SnO_2/$Cs_2AgBiBr_6$/P3HT/Au	1.04	1.78	78.00	1.44	[244]
FTO/TiO_2/$Rb_3Sb_2I_9$/Poly-TPD/Au	0.55	2.11	56.97	0.66	[245]
ITO/SnO_2/C60/ $FASnI_3$+SnF_2+TMA/Spiro-OMeTAD/Ag	0.31	21.65	64.70	4.34	[246]
ITO/cl-TiO_2/$Cs_2AgBiBr_6$/Spiro-OMeTAD/Au	1.06	1.55	74.00	1.22	[247]
FTO/b-TiO_2/n-TiO_2/$CH_3NH_3SnCl_3$/ PEO:KI/I_2/Pt	0.60	1.50	59.00	0.55	[248]
ITO/Cu-NiO/$Cs_2AgBiBr_6$/C_{60}/BCP/Ag	1.01	3.19	69.2	2.23	[249]
ITO/PEDOT:PSS/MASnIBr/$PC_{61}BM$ /Al	0.48	17.8	52.00	4.45	[250]
ITO/PEDOT:PSS/$FASnI_3$/$PC_{71}BM$/Ag	0.55	22.72	71.2	8.90	[251]
ITO/ PEDOT:PSS/$FA_{0.8}GA_{0.2}SnI_3$ (3D/2D)/C60/BCP/Ag anilinium solvent in the second step	0.64	21.10	76.30	10.40	[252]
FTO/PEDOT:PSS/FPSGI (7.5Ge)/BCP/Ag/Au	0.46	21.92	73.00	7.45	[253]

(continued)

Table 2 (continued)

Architecture	V_{OC} (V)	J_{SC} (mA cm^{-2})	FF (%)	PCE (%)	References
ITO/PEDOT:PSS/$FA_{0.75}MA_{0.25}SnI_3$/C_{60}/Ag	0.55	19.4	67.00	7.20	[254]
FTO/Cu-NiOx/$FASnI_3$/PCBM/Ag	0.69	21.15	74.00	10.86	[255]
ITO/PEDOT:PSS/$MA_3Bi_2I_9$/C_{60}/BCP/Ag	0.83	1.39	34.00	0.39	[256]
FTO/ PEDOT:PSS/GeI_2 doped $(FA0_{.9}EA_{0.1})_{0.98}EDA_{0.01}SnI_3$/$C_{60}$/BCP/Ag/Au	0.84	20.32	78.00	13.24	[49]
ITO/PEDOT:PSS/$MA_{0.8}HA_{0.2}SnI_3$/PCBM/Al	0.35	11.80	50.00	2.10	[99]
ITO/PEDOT:PSS/$MA_3Sb_2I_9$+HI/$PC_{71}BM$/C_{60}/BCP/Al	0.62	5.41	60.82	2.04	[257]
ITO/PEDOT:PSS/$GA_{0.2}FA_{0.78}SnI_3$-1%$EDAI_2$/C60 (20 nm)/BCP/Ag	0.562	20.80	72.60	8.50	[258]

contrast to photovoltaic technologies such as silicon, the performance estimation during the tests could be affected by the performance loss reversibility under day-night cycles [281] and hysteresis effects in the I-V curve [282].

Accordingly, it is possible to find different strategies to improve the lifetime, including alteration of their compositions and dimensionality, interfaces passivation [283], selective charge contacts [284], barrier designs [285], among other strategies. Thus, due that the electrodes and active areas of photovoltaic cells must be protected from ambient exposure conditions, it is mandatory that the strategies used to improve the lifetime are complemented by a proper device encapsulation or external barrier layer to mitigate corrosion processes, increase the electrical insulation, and provide mechanical support [286].

In this regard, it is worth noting that different encapsulating materials and techniques have been used in Perovskite solar devices [287]. For instance, ethylene–vinyl acetate (EVA) as encapsulant was successfully tested following the temperature cycles test suggested by IEC 61,215 [288]. Polyisobutylene (PIB) as a barrier layer shown promising results when the devices were tested in thermal cycles and Damp heat tests [289]. A similar approach using carbon layer as a barrier was probed in solar cells and minimodules, encapsulating the devices with additional glass and epoxy glue, increasing the long stability of devices up to 12,000 h of exposure under continuous illumination of one sun [290]. Besides, several epoxy resins have been tested as encapsulant material to evaluate the outdoor performance of minimodules of perovskite [148, 291].

Although a lot of work has been done on this topic [271, 272, 274], it is important to highlight that there is still a long way to go, particularly regarding incorporation or adaptation of international standards such as IEC 61,215 to evaluate the encapsulation process and improve the lifetime. On the other hand, due that this technology is in its infancy, and there are few statistical data available for large devices operated outdoors [148, 292, 293] it is necessary the outdoor evaluation in order to gain insights related to the stability or degradation processes of this emerging technology [293].

(b) Toxicity

As is well-known, the most perovskite-based devices were developed using a lead-based matrix. However, there is very strict legislation regarding the use of lead, especially due to their high toxicity [53], but these rules make an exception for lead that is used in the solders of conventional photovoltaic modules as well as in other electronic components. This toxicity makes it difficult to accept the technology and may conflict with the ESG Environmental, Social and Governance) policy that has been sought after worldwide [45]. In this regard, more recently, has been developed lead-free halide perovskites [37, 44, 97, 138]. The most viable substitutes for Pb are Sn and Ge, however, the biggest problem with these metals is that they already have chemical instability in the required oxidation state (2+), resulting in a perovskite with lower stability [166, 269, 294–297]. Sn is the metal that has received the most attention [97, 138, 298] to replace Pb, however, studies [138] have revealed an easy oxidation of

Sn^{2+}, with an n-type semiconductor behavior, to Sn^{4+}, whose behavior becomes that of a p-type semiconductor, which acts as a dopant inside the material, in a process called self-doping. Meanwhile, despite its toxicity, Pb has greater protection against oxidation. The first work using Sn replacing Pb in perovskite was reported by Hao et al. [238], in early 2014. The authors achieved an efficiency of 5.73% with $MASnI_3$ perovskite. In the same year, Hao et al. [299], using a methylammonium perovskite with a mixture of lead and tin ($CH_3NH_3Sn_{(1-x)}Pb_{(x)}I_3$), and Noel et al. [299], with a study of different solvents in the crystallization of perovskite, they achieved similar efficiencies—5.44 and 6.4%, respectively. Thus, other studies have been carried out in order to improve the stability of perovskite solar cells. However, these are recent studies and not fully understood, requiring intensification of studies for possible practical commercial applications of the devices [300].

(c) Upscaling

There are a number of problems that are caused in perovskite cells with increasing size, since larger areas can bring uniformity and morphology problems [301]. It is necessary to manufacture devices on an industrial scale, making the transition from a laboratory scale to a manufacturing scale [302]. Currently, most studies in the literature are limited to small areas (<1 cm^2), but devices to photovoltaic commercial sizes (>1 m^2) must be achieved [154].

Although different techniques have widely been used to fabricate metal-halide perovskite-based devices on larger areas (e.g., such as Doctor blade, Slot-die, Screen printing, and so on) [145], it is to highlight that spin-coting technique has been used successfully in areas up to 100 cm^2, obtaining the higher efficiencies [303]. This is an important aspect to remark, because 100 cm^2 of size is comparable with the size of silicon solar cells used in modules.

Accordingly, in order to improve the performance of perovskite technology beyond cells, the efforts are mainly focus on the cells interconnection passing from cells to, minimodules and modules [292, 304]. In this context, most of the perovskite devices are fabricated using three scribe lines or patterns (P1, P2, and P3) to interconnect the cells in series and mitigate electrical losses [292, 303, 305, 306]. This technique is widely employed in other thin-film photovoltaic technologies as silicon, CIGS, and polymer [307, 308]. In perovskite devices, P1 scribe line is performed on the transparent conductive oxide layer (ITO or FTO) to limit the sub-cells area. P2 scribe line is performed on the charge transport layers (electron and hole layers) and perovskite layer, intended to clear the ITO or FTO layer and allow interconnection between the back electrode and the charge transport layers. Finally, P3 scribe is performed to remove the back-contact layer and separate the cells. Therefore, the active area is limited by P1 and P3 lines. In contrast, the death-area is limited by P3 and P1 lines.

Consequently, the first certificated minimodule of this technology was reported in 2016 by SJTU team, which corresponded to 12.1% of efficiency, 10 serial cells, and an illuminated area of 36.13 cm^2 [309]. Nowadays, it is possible to find certified PSC module with an efficiency of 17.9% and 55 serial

cells [310]. This considerable progress in the up-scaling shows the effort of the community. Moreover, the multi-junctions with other photovoltaic technologies such as silicon and CIGS, opening new opportunities and challenges to be explored.

(d) Reproducibility

The more robust the synthesis, the more reproducible and less prone to small, subtle changes in the manufacturing process will the perovskite cells be. A robust process is important for reproducibility and scalability for large-scale manufacturing. These small variations in yield and conversion between synthesis batches when they are transferred to larger scales can generate huge losses, creating a certain risk associated with the implementation of large industrial plants. Undoubtedly, the reproducibility and the search for certification of measurements has been and will continue to be one of the biggest challenges for the establishment of perovskite solar cells [311, 312]. Here, it is important to mention that mesoporous structures in both architecture (p-i-n and n-i-p) helps to mitigate pin-holes improving the devices reproducibility. Besides the inverted mesoporous structure (ITO/NiO_x/Al_2O_3/MAPI/PCMB/Rhodamine/Au) has been demonstrated to be feasible for fabricating large-area devices up to 100 cm^2 in dry-box conditions by spin coating, improving the reproducibility and reducing hysteresis [147, 148]. Finally, the standardization of protocols for the fabrication of perovskite devices and ensuring reproducibility is highlighted.

5 Conclusions and Outlook

Overall, throughout this chapter, we have highlighted the enormous potential of the emerging metal-halide perovskites for photovoltaic applications. Certainly, the development of this technology will contribute to its popularization and sustainable use in the future. New manufacturing methods, device structure and materials continue to emerge. However, these emerging metal-halide perovskite devices still have several key aspects that need to be improved before their commercial application [313], allowing the introduction of a new and high-tech product on the market [314]. Finally, in this direction, more studies are needed to improve the stability of the devices and other problems still faced, so that it can reach commercialization in the coming years, including the use of new strategies such as Machine Learning [311, 315, 316] for database construction and prediction of the most promising synthesis routes to obtain the highest values of PCEs and ECEs.

Acknowledgements The authors gratefully acknowledge the support from the Brazilian agencies CAPES and CNPq.

References

1. Bisquert, J.: The Physics of Solar Energy Conversion, 1st edn. CRC Press (2020)
2. Green, M.A.: The path to 25% silicon solar cell efficiency: history of silicon cell evolution. Prog. Photovolt. Res. Appl. **17**(3), 183–189 (2009). https://doi.org/10.1002/PIP.892
3. Swanson, R.M.: Approaching the 29% limit efficiency of silicon solar cells. Conf. Rec. IEEE Photovolt. Spec. Conf. 889–894 (2005). https://doi.org/10.1109/PVSC.2005.1488274
4. Andreani, L.C., Bozzola, A., Kowalczewski, P., Liscidini, M., Redorici, L.: Silicon solar cells: toward the efficiency limits. Adv. Phys. X **4**(1), 1548305 (2018). https://doi.org/10.1080/23746149.2018.1548305
5. Ohnishi, M., Takeoka, A., Nakano, S., Kuwano, Y.: Advanced photovoltaic technologies and residential applications. Renew. Energy **6**(3), 275–282 (1995). https://doi.org/10.1016/0960-1481(95)00019-G
6. Raphael, E., Silva, M., Szostak, R., Schiavon, M.A., Nogueira, A.F.: células solares de perovskitas: uma nova tecnologia emergente. Quim. Nova (2017). https://doi.org/10.21577/0100-4042.20170127
7. Sun, C., et al.: Origins of hydrogen that passivates bulk defects in silicon heterojunction solar cells. Appl. Phys. Lett. **115**(25), 252103 (2019). https://doi.org/10.1063/1.5132368
8. Quansah, D.A., Adaramola, M.S.: Comparative study of performance degradation in poly- and mono-crystalline-Si solar PV modules deployed in different applications. Int. J. Hydrogen Energy **43**(6), 3092–3109 (2018). https://doi.org/10.1016/J.IJHYDENE.2017.12.156
9. Raphael, E., et al.: Células solares de perovskitas: uma nova tecnologia emergente. Quim. **41**(1), 61–74 (2018). https://doi.org/10.21577/0100-4042.20170127
10. Ling, J.K., et al.: A perspective on the commercial viability of perovskite solar cells. Sol. RRL **5**(11), 2100401 (2021). https://doi.org/10.1002/SOLR.202100401
11. Tailor, N.K., et al.: Recent progress in morphology optimization in perovskite solar cell. J. Mater. Chem. A **8**(41), 21356–21386 (2020). https://doi.org/10.1039/D0TA00143K
12. Chang, N.L., Ho-Baillie, A.W.Y., Vak, D., Gao, M., Green, M.A., Egan, R.J.: Manufacturing cost and market potential analysis of demonstrated roll-to-roll perovskite photovoltaic cell processes. Sol. Energy Mater. Sol. Cells **174**, 314–324 (2018). https://doi.org/10.1016/J.SOLMAT.2017.08.038
13. Moure, C., Peña, O.: Recent advances in perovskites: processing and properties. Prog. Solid State Chem. **43**(4), 123–148 (2015). https://doi.org/10.1016/J.PROGSOLIDSTCHEM.2015.09.001
14. Stranks, S.D., Snaith, H.J.: Metal-halide perovskites for photovoltaic and light-emitting devices. Nat. Nanotechnol. **10**(5), 391–402 (2015). https://doi.org/10.1038/nnano.2015.90
15. Manser, J.S., Christians, J.A., Kamat, P.V.: Intriguing optoelectronic properties of metal halide perovskites. Chem. Rev. **116**(21), 12956–13008 (2016). https://doi.org/10.1021/ACS.CHEMREV.6B00136
16. Di Girolamo, D., et al.: Dual effect of humidity on cesium lead bromide: enhancement and degradation of perovskite films. J. Mater. Chem. A **7**(19), 12292–12302 (2019). https://doi.org/10.1039/C9TA00715F
17. Mattoni, A., Meloni, S.: Defect dynamics in MAPbI3 polycrystalline films: the trapping effect of grain boundaries. Helv. Chim. Acta **103**(9), e2000110 (2020). https://doi.org/10.1002/HLCA.202000110
18. Cahen, D., Kronik, L., Hodes, G.: Are defects in lead-halide perovskites healed, tolerated, or both? ACS Energy Lett. **6**(11), 4108–4114 (2021). https://doi.org/10.1021/ACSENERGYLETT.1C02027
19. Phung, N., et al.: The role of grain boundaries on ionic defect migration in metal halide perovskites. Adv. Energy Mater. **10**(20), 1903735 (2020). https://doi.org/10.1002/AENM.201903735

20. Pinto, F.M., Suzuki, V.Y., Silva, R.C., La Porta, F.A.: Oxygen defects and surface chemistry of reducible oxides. Front. Mater. **6** (2019). https://doi.org/10.3389/fmats.2019.00260
21. Zhu, H., et al.: Screening in crystalline liquids protects energetic carriers in hybrid perovskites. Science (80-.) **353**(6306), 1409–1413 (2016). https://doi.org/10.1126/SCIENCE.AAF9570/SUPPL_FILE/ZHU.SM.PDF
22. Kojima, A., Teshima, K., Shirai, Y., Miyasaka, T.: Organometal halide perovskites as visible-light sensitizers for photovoltaic cells. J. Am. Chem. Soc. **131**(17), 6050–6051 (2009). https://doi.org/10.1021/ja809598r
23. Green, M., Dunlop, E., Hohl-Ebinger, J., Yoshita, M., Kopidakis, N., Hao, X.: Solar cell efficiency tables (version 57). Prog. Photovolt. Res. Appl. **29**(1), 3–15 (2021). https://doi.org/10.1002/PIP.3371
24. Rolston, N., et al.: Rapid open-air fabrication of perovskite solar modules. Joule **4**(12), 2675–2692 (2020). https://doi.org/10.1016/J.JOULE.2020.11.001
25. Tong, G., et al.: Scalable fabrication of >90 cm2 perovskite solar modules with >1000 h operational stability based on the intermediate phase strategy. Adv. Energy Mater. **11**(10), 2003712 (2021). https://doi.org/10.1002/AENM.202003712
26. Chen, H., et al.: A solvent- and vacuum-free route to large-area perovskite films for efficient solar modules. Nature **550**(7674), 92–95 (2017). https://doi.org/10.1038/nature23877
27. Wu, T., et al.: The main progress of perovskite solar cells in 2020–2021. Nano-Micro Lett. **13**(1), 1–18 (2021). https://doi.org/10.1007/S40820-021-00672-W/TABLES/1
28. Sahoo, S.., Manoharan, B., Sivakumar, N.: Introduction. In: Perovskite Photovoltaics, pp. 1–24. Elsevier (2018)
29. Best Research-Cell Efficiency Chart (2022). https://www.nrel.gov/pv/cell-efficiency.htm
30. Green, M.A., Dunlop, E.D., Hohl-Ebinger, J., Yoshita, M., Kopidakis, N., Hao, X.: Solar cell efficiency tables (version 59). Prog. Photovolt. Res. Appl. **30**(1), 3–12 (2022). https://doi.org/10.1002/pip.3506
31. Li, D., et al.: A review on scaling up perovskite solar cells. Adv. Funct. Mater. **31**(12), 2008621 (2021). https://doi.org/10.1002/ADFM.202008621
32. Correa-Baena, J.P., et al.: Promises and challenges of perovskite solar cells. Science (80-.) **358**(6364), 739–744 (2017). https://doi.org/10.1126/SCIENCE.AAM6323/SUPPL_FILE/AAM6323_CORREA-BAENA_SM.PDF
33. Rong, Y., et al.: Challenges for commercializing perovskite solar cells. Science (80-.) **361**(6408) (2018). https://doi.org/10.1126/SCIENCE.AAT8235/ASSET/FA0D3D3C-9EC5-44B8-A024-C9EC9D4B5244/ASSETS/GRAPHIC/361_AAT8235_FA.JPEG
34. Saliba, M., et al.: How to make over 20% efficient perovskite solar cells in regular (n-i-p) and inverted (p-i-n) architectures. Chem. Mater. **30**(13), 4193–4201 (2018). https://doi.org/10.1021/ACS.CHEMMATER.8B00136/SUPPL_FILE/CM8B00136_SI_004.MPG
35. Mei, A., et al.: A hole-conductor-free, fully printable mesoscopic perovskite solar cell with high stability. Science (80-.) **345**(6194), 295–298 (2014). https://doi.org/10.1126/SCIENCE.1254763/SUPPL_FILE/MEI.SM.PDF
36. Shi, T., et al.: Low-temperature fabrication of carbon-electrode based, hole-conductor-free and mesoscopic perovskite solar cells with power conversion efficiency > 12% and storage-stability > 220 days. Appl. Phys. Lett. **117**(16), 163501 (2020). https://doi.org/10.1063/5.0025442
37. Wang, R., Wang, J., Tan, S., Duan, Y., Wang, Z.K., Yang, Y.: Opportunities and challenges of lead-free perovskite optoelectronic devices. Trends Chem. **1**(4), 368–379 (2019). https://doi.org/10.1016/J.TRECHM.2019.04.004
38. Yang, S., Fu, W., Zhang, Z., Chen, H., Li, C.Z.: Recent advances in perovskite solar cells: efficiency, stability and lead-free perovskite. J. Mater. Chem. A **5**(23), 11462–11482 (2017). https://doi.org/10.1039/C7TA00366H

39. Giustino, F., Snaith, H.J.: Toward lead-free perovskite solar cells. ACS Energy Lett. **1**(6), 1233–1240 (2016). https://doi.org/10.1021/ACSENERGYLETT.6B00499
40. Shi, Z., et al.: Lead-free organic-inorganic hybrid perovskites for photovoltaic applications: recent advances and perspectives. Adv. Mater. **29**(16), 1605005 (2017). https://doi.org/10.1002/ADMA.201605005
41. Hailegnaw, B., Kirmayer, S., Edri, E., Hodes, G., Cahen, D.: Rain on methylammonium lead iodide based perovskites: possible environmental effects of perovskite solar cells. J. Phys. Chem. Lett. **6**(9), 1543–1547 (2015). https://doi.org/10.1021/ACS.JPCLETT.5B00504/SUPPL_FILE/JZ5B00504_SI_001.PDF
42. Kely, A., Souza, R., Morassuti, C.Y., Batista De Deus, W.: Poluição do ambiente por metais pesados e utilização de vegetais como bioindicadores. Acta Biomed. Bras. **9**(3), 95–106 (2018). https://doi.org/10.18571/ACBM.189
43. Von Sperling, M.: ntrodução à Qualidade das Águas e ao Tratamento de Esgotos, 4th edn. Editora UFMG (2014)
44. Wang, Q., Abate, A.: Perovskite solar cells : promises and challenges. In: Kurinec, S.K. (Ed.) Emerging Photovoltaic Materials: Silicon & Beyond, 1st edn, pp. 261–356. Scrivener Publishing, Beverly, USA (2019)
45. Li, J., et al.: Biological impact of lead from halide perovskites reveals the risk of introducing a safe threshold. Nat. Commun. **11**(310), 1–5 (2020). https://doi.org/10.1038/s41467-019-13910-y
46. Joshi, R.L.: Environmental science. J. Nepal Med. Assoc. **10**(3), 147–154 (2003). https://doi.org/10.31729/jnma.1240
47. Yue, S., et al.: Synthesis, characterization, and stability studies of Ge-based perovskites of controllable mixed cation composition, produced with an ambient surfactant-free approach. ACS Omega **4**(19), 18219–18233 (2019). https://doi.org/10.1021/ACSOMEGA.9B02203/SUPPL_FILE/AO9B02203_SI_001.PDF
48. Veronese, A., Patrini, M., Bajoni, D., Ciarrocchi, C., Quadrelli, P., Malavasi, L.: Highly tunable emission by halide engineering in lead-free perovskite-derivative nanocrystals: the Cs2SnX6 (X = Cl, Br, Br/I, I) system. Front. Chem. **8**, 35 (2020). https://doi.org/10.3389/FCHEM.2020.00035/BIBTEX
49. Nishimura, K., et al.: Lead-free tin-halide perovskite solar cells with 13% efficiency. Nano Energy **74**, 104858 (2020). https://doi.org/10.1016/J.NANOEN.2020.104858
50. Li, X.L., Li, Z., Zhang, G., Yang, G.J.: Lead-free perovskite [H3NC6H4NH3]CuBr 4 with both a bandgap of 1.43 eV and excellent stability. J. Mater. Chem. A **8**(11), 5484–5488 (2020). https://doi.org/10.1039/C9TA12872G
51. Arul, N.S., Nithya, V.D. (Eds.): Revolution of Perovskite. Springer Singapore, Singapore (2020)
52. Huang, Y.T., Kavanagh, S.R., Scanlon, D.O., Walsh, A., Hoye, R.L.Z.: Perovskite-inspired materials for photovoltaics and beyond—from design to devices. Nanotechnology **32**(13), 132004 (2021). https://doi.org/10.1088/1361-6528/ABCF6D
53. Pinto, F.M., Dey, S., Duarte, T.M., Taft, C.A., La Porta, F.A.: Perovskite-like quantum dots designed for advanced optoelectronic applications. In: de A. Taft, F., La Porta, C.A. (Eds.) Functional Properties of Advanced Engineering Materials and Biomolecules, 1st edn, pp. 83–108. Springer, Cham (2021)
54. Hong, X.: Nitride perovskite becomes polar. Science (80-.) **374**(6574), 1445–1446 (2021). https://doi.org/10.1126/science.abm7179
55. Mazzo, T.M., et al.: Controlling the electronic, structural, and optical properties of novel MgTiO 3/LaNiO 3 nanostructured films for enhanced optoelectronic devices. ACS Appl. Nano Mater. **2**(5), 2612–2620 (2019). https://doi.org/10.1021/acsanm.8b02110

56. Sato, T., Noréus, D., Takeshita, H., Häussermann, U.: Hydrides with the perovskite structure: general bonding and stability considerations and the new representative CaNiH3. J. Solid State Chem. **178**(11), 3381–3388 (2005). https://doi.org/10.1016/j.jssc.2005.08.026
57. Surucu, G., Gencer, A., Candan, A., Gullu, H.H., Isik, M.: CaXH 3 (X = Mn, Fe, Co) perovskite-type hydrides for hydrogen storage applications. Int. J. Energy Res. **44**(3), 2345–2354 (2020). https://doi.org/10.1002/er.5062
58. Flores-Livas, J.A., Sarmiento-Pérez, R., Botti, S., Goedecker, S., Marques, M.A.L.: Rare-earth magnetic nitride perovskites. J. Phys. Mater. **2**(2), 025003 (2019). https://doi.org/10.1088/2515-7639/ab083e
59. Terranova, U., Viñes, F., de Leeuw, N.H., Illas, F.: Mechanisms of carbon dioxide reduction on strontium titanate perovskites. J. Mater. Chem. A **8**(18), 9392–9398 (2020). https://doi.org/10.1039/D0TA01502D
60. Assirey, E.A.R.: Perovskite synthesis, properties and their related biochemical and industrial application. Saudi Pharm. J. **27**(6), 817–829 (2019). https://doi.org/10.1016/j.jsps.2019.05.003
61. Borowski, M.: Perovskites: Structure. Nova Science Pub Inc., Properties and Uses (2011)
62. Nakata, M.M., Mazzo, T.M., Casali, G.P., La Porta, F.A., Longo, E.: A large red-shift in the photoluminescence emission of Mg 1–x Sr x TiO 3. Chem. Phys. Lett. **622**, 9–14 (2015). https://doi.org/10.1016/j.cplett.2015.01.011
63. Fuertes, A.: Nitride tuning of transition metal perovskites. APL Mater. **8**(2), 020903 (2020). https://doi.org/10.1063/1.5140056
64. Oliveira, L.H., et al.: Optical and gas-sensing properties, and electronic structure of the mixed-phase CaCu 3 Ti 4 O 12 /CaTiO 3 composites. Mater. Res. Bull. **93**, 47–55 (2017). https://doi.org/10.1016/j.materresbull.2017.04.037
65. Schouwink, P., et al.: Structure and properties of complex hydride perovskite materials. Nat. Commun. **5**(1), 5706 (2014). https://doi.org/10.1038/ncomms6706
66. Lin, N., Gong, Y., Wang, R., Wang, Y., Zhang, X.: Critical review of perovskite-based materials in advanced oxidation system for wastewater treatment: design, applications and mechanisms. J. Hazard. Mater. **424**, 127637 (2022). https://doi.org/10.1016/j.jhazmat.2021.127637
67. Chouhan, L., Ghimire, S., Subrahmanyam, C., Miyasaka, T., Biju, V.: Synthesis, optoelectronic properties and applications of halide perovskites. Chem. Soc. Rev. **49**(10), 2869–2885 (2020). https://doi.org/10.1039/C9CS00848A
68. Ha, S.-T., Su, R., Xing, J., Zhang, Q., Xiong, Q.: Metal halide perovskite nanomaterials: synthesis and applications. Chem. Sci. **8**(4), 2522–2536 (2017). https://doi.org/10.1039/C6SC04474C
69. Thomas, A., Thankappan, S.: Perovskite Photovoltaics: Basic to Advanced Concepts and Implementation. Academic Press (2018)
70. Xu, W., et al.: Rational molecular passivation for high-performance perovskite light-emitting diodes. Nat. Photon. **13**(6), 418–424 (2019). https://doi.org/10.1038/s41566-019-0390-x
71. Yakunin, S., et al.: Low-threshold amplified spontaneous emission and lasing from colloidal nanocrystals of caesium lead halide perovskites. Nat. Commun. **6**(1), 8056 (2015). https://doi.org/10.1038/ncomms9056
72. Jena, A.K., Kulkarni, A., Miyasaka, T.: Halide perovskite photovoltaics: background, status, and future prospects. Chem. Rev. **119**(5), 3036–3103 (2019). https://doi.org/10.1021/acs.chemrev.8b00539
73. Protesescu, L., et al.: Nanocrystals of cesium lead halide perovskites (CsPbX 3, X = Cl, Br, and I): novel optoelectronic materials showing bright emission with wide color gamut. Nano Lett. **15**(6), 3692–3696 (2015). https://doi.org/10.1021/nl5048779
74. Park, N.-G., Grätzel, M., Miyasaka, T. (eds.): Organic-Inorganic Halide Perovskite Photovoltaics. Springer International Publishing, Cham (2016)
75. Quarti, C., Katan, C., Even, J.: Physical properties of bulk, defective, 2D and 0D metal halide perovskite semiconductors from a symmetry perspective. J. Phys. Mater. **3**(4), 042001 (2020). https://doi.org/10.1088/2515-7639/aba6f6

76. Zhou, Y., Zhao, Y.: Chemical stability and instability of inorganic halide perovskites. Energy Environ. Sci. **12**(5), 1495–1511 (2019). https://doi.org/10.1039/C8EE03559H
77. Frost, J.M., Walsh, A.: Molecular motion and dynamic crystal structures of hybrid halide perovskites. In: Organic-Inorganic Halide Perovskite Photovoltaics. Springer International Publishing, Cham, pp. 1–17 (2016)
78. Glazer, A.M.: The classification of tilted octahedra in perovskites. Acta Crystallogr. Sect. B Struct. Crystallogr. Cryst. Chem. **28**(11), 3384–3392 (1972). https://doi.org/10.1107/S0567740872007976
79. Halcrow, M.A.: Jahn–Teller distortions in transition metal compounds, and their importance in functional molecular and inorganic materials. Chem. Soc. Rev. **42**(4), 1784–1795 (2013). https://doi.org/10.1039/C2CS35253B
80. Ullmann, H., Trofimenko, N.: Estimation of effective ionic radii in highly defective perovskite-type oxides from experimental data. J. Alloys Compd. **316**(1–2), 153–158 (2001). https://doi.org/10.1016/S0925-8388(00)01448-1
81. Steele, J.A. et al.: Thermal unequilibrium of strained black CsPbI 3 thin films. Science (80-.) **365**(6454), 679–684 (2019). https://doi.org/10.1126/science.aax3878
82. Meggiolaro, D., et al.: Iodine chemistry determines the defect tolerance of lead-halide perovskites. Energy Environ. Sci. **11**(3), 702–713 (2018). https://doi.org/10.1039/C8EE00124C
83. Shamsi, J., Urban, A.S., Imran, M., De Trizio, L., Manna, L.: Metal halide perovskite nanocrystals: synthesis, post-synthesis modifications, and their optical properties. Chem. Rev. **119**(5), 3296–3348 (2019). https://doi.org/10.1021/acs.chemrev.8b00644
84. Jing, Q., Xu, Y., Su, Y., Xing, X., Lu, Z.: A systematic study of the synthesis of cesium lead halide nanocrystals: does Cs 4 PbBr 6 or CsPbBr 3 form? Nanoscale **11**(4), 1784–1789 (2019). https://doi.org/10.1039/C8NR08116F
85. Brivio, F., Walker, A.B., Walsh, A.: Structural and electronic properties of hybrid perovskites for high-efficiency thin-film photovoltaics from first-principles. APL Mater. **1**(4), 042111 (2013). https://doi.org/10.1063/1.4824147
86. Goldschmidt, V.M.: Die gesetze der krystallochemie. Naturwissenschaften **14**(21), 477–485 (1926). https://doi.org/10.1007/BF01507527
87. Zhang, H., Li, N., Li, K., Xue, D.: Structural stability and formability of AB O 3 -type perovskite compounds. Acta Crystallogr. Sect. B Struct. Sci. **63**(6), 812–818 (2007). https://doi.org/10.1107/S0108768107046174
88. Li, C., Lu, X., Ding, W., Feng, L., Gao, Y., Guo, Z.: Formability of ABX 3 (X = F, Cl, Br, I) halide perovskites. Acta Crystallogr. Sect. B Struct. Sci. **64**(6), 702–707 (2008). https://doi.org/10.1107/S0108768108032734
89. Bartel, C.J., et al.: New tolerance factor to predict the stability of perovskite oxides and halides. Sci. Adv. **5**(2) (2019). https://doi.org/10.1126/sciadv.aav0693
90. Rao, C.N.R.: Perovskites. In: Encyclopedia of Physical Science and Technology, pp. 707–714. Elsevier (2003)
91. Akkerman, Q.A., Manna, L.: What defines a halide perovskite? ACS Energy Lett. **5**(2), 604–610 (2020). https://doi.org/10.1021/acsenergylett.0c00039
92. Zhou, C., Lin, H., Lee, S., Chaaban, M., Ma, B.: Organic–inorganic metal halide hybrids beyond perovskites. Mater. Res. Lett. **6**(10), 552–569 (2018). https://doi.org/10.1080/21663831.2018.1500951
93. Adjogri, S.J., Meyer, E.L.: A review on lead-free hybrid halide perovskites as light absorbers for photovoltaic applications based on their structural, optical, and morphological properties. Molecules **25**(21), 5039 (2020). https://doi.org/10.3390/molecules25215039
94. Xiao, Z., Song, Z., Yan, Y.: From lead halide perovskites to lead-free metal halide perovskites and perovskite derivatives. Adv. Mater. **31**(47), 1803792 (2019). https://doi.org/10.1002/adma.201803792

95. Gu, S., Lin, R., Han, Q., Gao, Y., Tan, H., Zhu, J.: Tin and mixed lead–tin halide perovskite solar cells: progress and their application in tandem solar cells. Adv. Mater. 1907392 (2020). https://doi.org/10.1002/adma.201907392
96. Savill, K.J., Ulatowski, A.M., Herz, L.M.: Optoelectronic properties of tin-lead halide perovskites. ACS Energy Lett. **6**(7), 2413–2426 (2021). https://doi.org/10.1021/acsenergylett.1c00776
97. Hoefler, S.F., Trimmel, G., Rath, T.: Progress on lead-free metal halide perovskites for photovoltaic applications: a review. Monatshefte fur Chemie **148**(5), 795–826 (2017). https://doi.org/10.1007/s00706-017-1933-9
98. Filip, M.R., Giustino, F.: Computational screening of homovalent lead substitution in organic-inorganic halide perovskites. J. Phys. Chem. C **120**(1), 166–173 (2016). https://doi.org/10.1021/acs.jpcc.5b11845
99. Tsarev, S., et al.: Hydrazinium-assisted stabilisation of methylammonium tin iodide for lead-free perovskite solar cells. J. Mater. Chem. A **6**(43), 21389–21395 (2018). https://doi.org/10.1039/C8TA07699E
100. Shockley, W., Queisser, H.J.: Detailed balance limit of efficiency of p-n junction solar cells. J. Appl. Phys. **32**(3), 510–519 (1961). https://doi.org/10.1063/1.1736034
101. Fan, Q., et al.: Lead-free halide perovskite nanocrystals: crystal structures, synthesis, stabilities, and optical properties. Angew. Chemie Int. Ed. **59**(3), 1030–1046 (2020). https://doi.org/10.1002/anie.201904862
102. Kour, R., et al.: Potential substitutes for replacement of lead in perovskite solar cells: a review. Glob. Challenges **3**(11), 1900050 (2019). https://doi.org/10.1002/gch2.201900050
103. Filip, M.R., Volonakis, G., Giustino, F.: Hybrid halide perovskites: fundamental theory and materials design. In: Handbook of Materials Modeling. Springer International Publishing, Cham, pp. 1–30 (2018)
104. Muscarella, L.A., et al.: Air-stable and oriented mixed lead halide perovskite (FA/MA) by the one-step deposition method using zinc iodide and an alkylammonium additive. ACS Appl. Mater. Interfaces **11**(19), 17555–17562 (2019). https://doi.org/10.1021/acsami.9b03810
105. Men, L., Rosales, B.A., Gentry, N.E., Cady, S.D., Vela, J.: Lead-free semiconductors: soft chemistry, dimensionality control, and manganese-doping of germanium halide perovskites. ChemNanoMat **5**(3), 334–339 (2019). https://doi.org/10.1002/cnma.201800497
106. Sun, P.-P., Li, Q.-S., Yang, L.-N., Li, Z.-S.: Theoretical insights into a potential lead-free hybrid perovskite: substituting Pb 2+ with Ge 2+. Nanoscale **8**(3), 1503–1512 (2016). https://doi.org/10.1039/C5NR05337D
107. Chen, M., et al.: Highly stable and efficient all-inorganic lead-free perovskite solar cells with native-oxide passivation. Nat. Commun. **10**(1), 16 (2019). https://doi.org/10.1038/s41467-018-07951-y
108. Nagane, S., et al.: Lead-free perovskite semiconductors based on germanium-tin solid solutions: structural and optoelectronic properties. J. Phys. Chem. C **122**(11), 5940–5947 (2018). https://doi.org/10.1021/acs.jpcc.8b00480
109. Körbel, S., Marques, M.A.L., Botti, S.: Stability and electronic properties of new inorganic perovskites from high-throughput ab initio calculations. J. Mater. Chem. C **4**(15), 3157–3167 (2016). https://doi.org/10.1039/C5TC04172D
110. Hong, F., Saparov, B., Meng, W., Xiao, Z., Mitzi, D.B., Yan, Y.: Viability of lead-free perovskites with mixed chalcogen and halogen anions for photovoltaic applications. J. Phys. Chem. C **120**(12), 6435–6441 (2016). https://doi.org/10.1021/acs.jpcc.6b00920
111. Li, L., Dong, T.: Photoluminescence tuning in carbon dots: surface passivation or/and functionalization, heteroatom doping. J. Mater. Chem. C **6**(30), 7944–7970 (2018). https://doi.org/10.1039/C7TC05878K
112. Sun, Y.-Y., et al.: Discovering lead-free perovskite solar materials with a split-anion approach. Nanoscale **8**(12), 6284–6289 (2016). https://doi.org/10.1039/C5NR04310G

113. Yang, B., et al.: Lead-free silver-bismuth halide double perovskite nanocrystals. Angew. Chemie Int. Ed. **57**(19), 5359–5363 (2018). https://doi.org/10.1002/anie.201800660
114. Zhang, Q., Hao, F., Li, J., Zhou, Y., Wei, Y., Lin, H.: Perovskite solar cells: must lead be replaced—and can it be done? Sci. Technol. Adv. Mater. **19**(1), 425–442 (2018). https://doi.org/10.1080/14686996.2018.1460176
115. Volonakis, G., et al.: Lead-free halide double perovskites via heterovalent substitution of noble metals. J. Phys. Chem. Lett. **7**(7), 1254–1259 (2016). https://doi.org/10.1021/acs.jpclett.6b00376
116. Zhao, X.-G., et al.: Design of lead-free inorganic halide perovskites for solar cells via cation-transmutation. J. Am. Chem. Soc. **139**(7), 2630–2638 (2017). https://doi.org/10.1021/jacs.6b09645
117. Wei, F., et al.: The synthesis, structure and electronic properties of a lead-free hybrid inorganic–organic double perovskite (MA) 2 KBiCl 6 (MA = methylammonium). Mater. Horizons **3**(4), 328–332 (2016). https://doi.org/10.1039/C6MH00053C
118. Deng, Z., et al.: Synthesis and characterization of the rare-earth hybrid double perovskites: (CH 3 NH 3) 2 KGdCl 6 and (CH 3 NH 3) 2 KYCl 6. J. Phys. Chem. Lett. **8**(20), 5015–5020 (2017). https://doi.org/10.1021/acs.jpclett.7b02322
119. Zhao, S., Yamamoto, K., Iikubo, S., Hayase, S., Ma, T.: First-principles study of electronic and optical properties of lead-free double perovskites Cs2NaBX6 (B = Sb, Bi; X = Cl, Br, I). J. Phys. Chem. Solids **117**, 117–121 (2018). https://doi.org/10.1016/j.jpcs.2018.02.032
120. Meyer, G.: The synthesis and structures of complex rare-earth halides. Prog. Solid State Chem. **14**(3), 141–219 (1982). https://doi.org/10.1016/0079-6786(82)90005-X
121. Flerov, I.N., Gorev, M.V., Aleksandrov, K.S., Tressaud, A., Grannec, J., Couzi, M.: Phase transitions in elpasolites (ordered perovskites). Mater. Sci. Eng. R Rep. **24**(3), 81–151 (1998). https://doi.org/10.1016/S0927-796X(98)00015-1
122. Filip, M.R., Liu, X., Miglio, A., Hautier, G., Giustino, F.: Phase diagrams and stability of lead-free halide double perovskites Cs 2 BB′X 6: B = Sb and Bi, B′ = Cu, Ag, and Au, and X = Cl, Br, and I. J. Phys. Chem. C **122**(1), 158–170 (2018). https://doi.org/10.1021/acs.jpcc.7b10370
123. Xiao, Z., Du, K., Meng, W., Mitzi, D.B., Yan, Y.: Chemical origin of the stability difference between copper(I)- and silver(I)-based halide double perovskites. Angew. Chemie Int. Ed. **56**(40), 12107–12111 (2017). https://doi.org/10.1002/anie.201705113
124. Zhao, X.-G., Yang, D., Ren, J.-C., Sun, Y., Xiao, Z., Zhang, L.: Rational design of halide double perovskites for optoelectronic applications. Joule **2**(9), 1662–1673 (2018). https://doi.org/10.1016/j.joule.2018.06.017
125. Maughan, A.E., Ganose, A.M., Scanlon, D.O., Neilson, J.R.: Perspectives and design principles of vacancy-ordered double perovskite halide semiconductors. Chem. Mater. **31**(4), 1184–1195 (2019). https://doi.org/10.1021/acs.chemmater.8b05036
126. Maughan, A.E., Ganose, A.M., Bordelon, M.M., Miller, E.M., Scanlon, D.O., Neilson, J.R.: Defect tolerance to intolerance in the vacancy-ordered double perovskite semiconductors Cs 2 SnI 6 and Cs 2 TeI 6. J. Am. Chem. Soc. **138**(27), 8453–8464 (2016). https://doi.org/10.1021/jacs.6b03207
127. Dey, A., et al.: State of the art and prospects for halide perovskite nanocrystals. ACS Nano **15**(7), 10775–10981 (2021). https://doi.org/10.1021/acsnano.0c08903
128. Chang, J.-H., Doert, T., Ruck, M.: Structural variety of defect perovskite variants M 3 E 2 X 9 (M = Rb, Tl, E = Bi, Sb, X = Br, I). Zeitschrift für Anorg. und Allg. Chemie **642**(13), 736–748 (2016). https://doi.org/10.1002/zaac.201600179
129. Shen, Y., et al.: Lead-free, stable, high-efficiency (52%) blue luminescent FA 3 Bi 2 Br 9 perovskite quantum dots. Nanoscale Horizons **5**(3), 580–585 (2020). https://doi.org/10.1039/C9NH00685K

130. Leng, M., et al.: Surface passivation of bismuth-based perovskite variant quantum dots to achieve efficient blue emission. Nano Lett. **18**(9), 6076–6083 (2018). https://doi.org/10.1021/acs.nanolett.8b03090
131. Saparov, B., et al.: Thin-film preparation and characterization of Cs 3 Sb 2 I 9: a lead-free layered perovskite semiconductor. Chem. Mater. **27**(16), 5622–5632 (2015). https://doi.org/10.1021/acs.chemmater.5b01989
132. Pal, J., Manna, S., Mondal, A., Das, S., Adarsh, K.V., Nag, A.: Colloidal synthesis and photophysics of M 3 Sb 2 I 9 (M=Cs and Rb) nanocrystals: lead-free perovskites. Angew. Chemie Int. Ed. **56**(45), 14187–14191 (2017). https://doi.org/10.1002/anie.201709040
133. Chonamada, T.D., Dey, A.B., Santra, P.K.: Degradation studies of Cs 3 Sb 2 I 9: a lead-free perovskite. ACS Appl. Energy Mater. **3**(1), 47–55 (2020). https://doi.org/10.1021/acsaem.9b01899
134. Lee, B., et al.: Air-stable molecular semiconducting iodosalts for solar cell applications: Cs 2 SnI 6 as a hole conductor. J. Am. Chem. Soc. **136**(43), 15379–15385 (2014). https://doi.org/10.1021/ja508464w
135. Sakai, N., et al.: Solution-processed cesium hexabromopalladate(IV), Cs 2 PdBr 6, for optoelectronic applications. J. Am. Chem. Soc. **139**(17), 6030–6033 (2017). https://doi.org/10.1021/jacs.6b13258
136. Ju, M.-G., et al.: Earth-abundant nontoxic titanium(IV)-based vacancy-ordered double perovskite halides with tunable 1.0 to 1.8 ev bandgaps for photovoltaic applications. ACS Energy Lett. **3**(2), 297–304 (2018). https://doi.org/10.1021/acsenergylett.7b01167
137. López-Fraguas, E., Masi, S., Mora-Seró, I.: Optical characterization of lead-free Cs 2 SnI 6 double perovskite fabricated from degraded and reconstructed CsSnI 3 films. ACS Appl. Energy Mater. **2**(12), 8381–8387 (2019). https://doi.org/10.1021/acsaem.9b01827
138. Wang, X., Zhang, T., Lou, Y., Zhao, Y.: All-inorganic lead-free perovskites for optoelectronic applications. Mater. Chem. Front. **3**(3), 365–375 (2019). https://doi.org/10.1039/c8qm00611c
139. Umedov, S.T., Khadka, D.B., Yanagida, M., Grigorieva, A., Shirai, Y.: A-site tailoring in the vacancy-ordered double perovskite semiconductor Cs2SnI6 for photovoltaic application. Sol. Energy Mater. Sol. Cells **230**, 111180 (2021). https://doi.org/10.1016/j.solmat.2021.111180
140. Liu, S., et al.: A review on additives for halide perovskite solar cells. Adv. Energy Mater. **10**(13), 1–28 (2020). https://doi.org/10.1002/aenm.201902492
141. Petrus, M.L., et al.: Capturing the sun: a review of the challenges and perspectives of perovskite solar cells. Adv. Energy Mater. **7**(16), 1700264 (2017). https://doi.org/10.1002/AENM.201700264
142. Salim, T., Sun, S., Abe, Y., Krishna, A., Grimsdale, A.C., Lam, Y.M.: Perovskite-based solar cells: impact of morphology and device architecture on device performance. J. Mater. Chem. A **3**(17), 8943–8969 (2015). https://doi.org/10.1039/C4TA05226A
143. Burschka, J., et al.: Sequential deposition as a route to high-performance perovskite-sensitized solar cells. Nature 2013 4997458 **499**(7458), 316–319 (2013). https://doi.org/10.1038/nature12340
144. Vaynzof, Y., Vaynzof, Y.: The future of perovskite photovoltaics—thermal evaporation or solution processing? Adv. Energy Mater. **10**(48), 2003073 (2020). https://doi.org/10.1002/AENM.202003073
145. Park, N.G., Zhu, K.: Scalable fabrication and coating methods for perovskite solar cells and solar modules. Nat. Rev. Mater. **5**(5), 333–350 (2020). https://doi.org/10.1038/s41578-019-0176-2
146. Chaudhary, K.T.: Thin film deposition: solution based approach. Thin Film. (2021). https://doi.org/10.5772/INTECHOPEN.94455
147. Ramirez, D., Velilla, E., Montoya, J.F., Jaramillo, F.: Mitigating scalability issues of perovskite photovoltaic technology through a p-i-n meso-superstructured solar cell architecture. Sol. Energy Mater. Sol. Cells **195**, 191–197 (2019). https://doi.org/10.1016/J.SOLMAT.2019.03.014

148. Velilla, E., Ramirez, D., Uribe, J.I., Montoya, J.F., Jaramillo, F.: Outdoor performance of perovskite solar technology: Silicon comparison and competitive advantages at different irradiances. Sol. Energy Mater. Sol. Cells **191**, 15–20 (2019). https://doi.org/10.1016/J.SOLMAT.2018.10.018
149. Aguilar, R.G., Ortiz López, J.: Low cost instrumentation for spin-coating deposition of thin films in an undergraduate laboratory. Am. J. Phys. Educ. **5**(2), 368 (2011)
150. Hyuck Heo, J., Ho Song, D., Hyuk Im, S., Heo, J.H., Song, D.H., Im, S.H.: Planar CH3NH3PbBr3 hybrid solar cells with 10.4% power conversion efficiency, fabricated by controlled crystallization in the spin-coating process. Adv. Mater. **26**(48), 8179–8183 (2014). https://doi.org/10.1002/ADMA.201403140
151. Eslamian, M.: Inorganic and organic solution-processed thin film devices. Nano-Micro Lett. **9**(1), 1–23 (2016). https://doi.org/10.1007/S40820-016-0106-4
152. Stranks, S.D., Nayak, P.K., Zhang, W., Stergiopoulos, T., Snaith, H.J.: Formation of thin films of organic-inorganic perovskites for high-efficiency solar cells. Angew. Chemie Int. Ed. **54**(11), 3240–3248 (2015). https://doi.org/10.1002/ANIE.201410214
153. Huang, P.H., Wang, Y.H., Ke, J.C., Huang, C.J.: The effect of solvents on the performance of CH3NH3PbI3 perovskite solar cells. Energies **10**(5), 599 (2017). https://doi.org/10.3390/EN10050599
154. Howard, I.A., et al.: Coated and printed perovskites for photovoltaic applications. Adv. Mater. **31**(26), 1806702 (2019). https://doi.org/10.1002/ADMA.201806702
155. Stranks, S.D., Nayak, P.K., Zhang, W., Stergiopoulos, T., Snaith, H.J.: Formation of thin films of organic-inorganic perovskites for high-efficiency solar cells. Angew. Chemie—Int. Ed. **54**(11), 3240–3248 (2015). https://doi.org/10.1002/anie.201410214
156. El Cohen, B., Gamliel, S., Etgar, L.: Parameters influencing the deposition of methylammonium lead halide iodide in hole conductor free perovskite-based solar cells. APL Mater. **2**(8), 081502 (2014). https://doi.org/10.1063/1.4885548
157. Burschka, J., et al.: Sequential deposition as a route to high-performance perovskite-sensitized solar cells. Nature **499**, 316–319 (2013). https://doi.org/10.1038/nature12340
158. Zheng, L., et al.: Improved light absorption and charge transport for perovskite solar cells with rough interfaces by sequential deposition. Nanoscale **6**, 8171–8176 (2014). https://doi.org/10.1039/c4nr01141d
159. Yoo, S.M., et al.: Preparation of nanoscale inorganic CsPbIxBr 3–x perovskite photosensitizers on the surface of mesoporous TiO2 film for solid-state sensitized solar cells. Appl. Surf. Sci. **551**, 149387 (2021). https://doi.org/10.1016/J.APSUSC.2021.149387
160. Yoo, S.M., et al.: Nanoscale perovskite-sensitized solar cell revisited: dye-cell or perovskite-cell? Chemsuschem **13**(10), 2571–2576 (2020). https://doi.org/10.1002/CSSC.202000223
161. Lee, J.W., Park, N.G.: Two-step deposition method for high-efficiency perovskite solar cells. MRS Bull. **40**(8), 654–659 (2015). https://doi.org/10.1557/MRS.2015.166
162. Chen, H.: Two-step sequential deposition of organometal halide perovskite for photovoltaic application. Adv. Funct. Mater. **27**(8), 1605654 (2017). https://doi.org/10.1002/ADFM.201605654
163. Gonzalez-Pedro, V., et al.: General working principles of CH3NH3PbX3 perovskite solar cells. Nano Lett. **14**(2), 888–893 (2014). https://doi.org/10.1021/NL404252E/SUPPL_FILE/NL404252E_SI_001.PDF
164. Kim, J.S., Cho, H., Wolf, C., Yun, H.J., Heo, J.M., Lee, T.W.: Increased luminescent efficiency of perovskite light emitting diodes based on modified two-step deposition method providing gradient concentration. APL Mater. **6**(11), 111101 (2018). https://doi.org/10.1063/1.5047456
165. Geon Lee, D., et al.: High efficiency perovskite solar cells exceeding 22% via a photo-assisted two-step sequential deposition. Adv. Funct. Mater. **31**(9), 2006718 (2021). https://doi.org/10.1002/ADFM.202006718

166. Saki, Z., Byranvand, M.M., Taghavinia, N., Kedia, M., Saliba, M.: Solution-processed perovskite thin-films: the journey from lab: the large-scale solar cells. Energy Environ. Sci. **14**(11), 5690–5722 (2021). https://doi.org/10.1039/d1ee02018h
167. Ghosh, S., Mishra, S., Singh, T.: Antisolvents in perovskite solar cells: importance, issues, and alternatives. Adv. Mater. Interfaces **7**(18), 2000950 (2020). https://doi.org/10.1002/ADMI.202000950
168. Guo, Y., et al.: Chemical pathways connecting lead(II) iodide and perovskite via polymeric plumbate(II) fiber. J. Am. Chem. Soc. **137**(50), 15907–15914 (2015). https://doi.org/10.1021/JACS.5B10599/SUPPL_FILE/JA5B10599_SI_006.CIF
169. Xiao, S., et al.: Unveiling a key intermediate in solvent vapor postannealing to enlarge crystalline domains of organometal halide perovskite films. Adv. Funct. Mater. **27**(12), 1604944 (2017). https://doi.org/10.1002/ADFM.201604944
170. Zhang, K., et al.: A prenucleation strategy for ambient fabrication of perovskite solar cells with high device performance uniformity. Nat. Commun. **11**(1), 1–11 (2020). https://doi.org/10.1038/s41467-020-14715-0
171. Ahmadian-Yazdi, M.R., Zabihi, F., Habibi, M., Eslamian, M.: Effects of process parameters on the characteristics of mixed-halide perovskite solar cells fabricated by one-step and two-step sequential coating. Nanoscale Res. Lett. **11**(1) (2016). https://doi.org/10.1186/s11671-016-1601-8
172. Ren, Y., et al.: New insight into solvent engineering technology from evolution of intermediates via one-step spin-coating approach. Sci. China Mater. **60**(5), 392–398 (2017). https://doi.org/10.1007/s40843-017-9027-1
173. Jeon, N.J., Noh, J.H., Kim, Y.C., Yang, W.S., Ryu, S., Il Seok, S.: Solvent engineering for high-performance inorganic-organic hybrid perovskite solar cells. Nat. Mater. **13**(9), 897–903 (2014). https://doi.org/10.1038/nmat4014
174. Pascoe, A.R., et al.: Enhancing the Optoelectronic performance of perovskite solar cells via a textured CH3NH3PbI3 morphology. Adv. Funct. Mater. **26**(8), 1278–1285 (2016). https://doi.org/10.1002/ADFM.201504190
175. Xiao, M., et al.: A fast deposition-crystallization procedure for highly efficient lead iodide perovskite thin-film solar cells. Angew. Chemie Int. Ed. **53**(37), 9898–9903 (2014). https://doi.org/10.1002/ANIE.201405334
176. Xiao, Z., et al.: Solvent annealing of perovskite-induced crystal growth for photovoltaic-device efficiency enhancement. Adv. Mater. **26**(37), 6503–6509 (2014). https://doi.org/10.1002/ADMA.201401685
177. World Energy Outlook 2019—Analysis—IEA
178. Zissis, G.: Energy consumption and environmental and economic impact of lighting: the current situation. Handb. Adv. Light. Technol. 1–13 (2016). https://doi.org/10.1007/978-3-319-00295-8_40-1
179. Luo, J., Hu, M., Niu, G., Tang, J.: Lead-free halide perovskites and perovskite variants as phosphors toward light-emitting applications. ACS Appl. Mater. Interfaces **11**(35), 31575–31584 (2019). https://doi.org/10.1021/ACSAMI.9B08407
180. Mandil, C.: Light's labour's lost: policies for energy-efficient lighting. Energy world **343**, 14–15 (2006)
181. Jaramillo-Quintero, O.A., Sanchez, R.S., Rincon, M., Mora-Sero, I.: Bright visible-infrared light emitting diodes based on hybrid halide perovskite with spiro-OMeTAD as a hole-injecting layer. J. Phys. Chem. Lett. **6**(10), 1883–1890 (2015). https://doi.org/10.1021/ACS.JPCLETT.5B00732/SUPPL_FILE/JZ5B00732_SI_001.PDF
182. Sanchez, R.S., De La Fuente, M.S., Suarez, I., Muñoz-Matutano, G., Martinez-Pastor, J.P., Mora-Sero, I.: Tunable light emission by exciplex state formation between hybrid halide perovskite and core/shell quantum dots: Implications in advanced LEDs and photovoltaics. Sci. Adv. **2**(1) (2016). https://doi.org/10.1126/sciadv.1501104

183. Yang, B., et al.: Lead-free, air-stable all-inorganic cesium bismuth halide perovskite nanocrystals. Angew. Chemie—Int. Ed. **56**(41), 12471–12475 (2017). https://doi.org/10.1002/anie.201704739
184. Sun, Q., Wang, J., Yin, W.J., Yan, Y.: Bandgap engineering of stable lead-free oxide double perovskites for photovoltaics. Adv. Mater. **30**(15), 1–9 (2018). https://doi.org/10.1002/adma.201705901
185. Wang, X., Li, T., Xing, B., Faizan, M., Biswas, K., Zhang, L.: Metal halide semiconductors beyond lead-based perovskites for promising optoelectronic applications. J. Phys. Chem. Lett. **12**(43), 10532–10550 (2021). https://doi.org/10.1021/ACS.JPCLETT.1C02877
186. Zheng, X., Hou, Y., Sun, H.T., Mohammed, O.F., Sargent, E.H., Bakr, O.M.: Reducing defects in halide perovskite nanocrystals for light-emitting applications. J. Phys. Chem. Lett. **10**(10), 2629–2640 (2019). https://doi.org/10.1021/ACS.JPCLETT.9B00689
187. Dequilettes, D.W., et al.: Charge-carrier recombination in halide perovskites. Chem. Rev. **119**(20), 11007–11019 (2019). https://doi.org/10.1021/ACS.CHEMREV.9B00169/SUPPL_FILE/CR9B00169_SI_001.PDF
188. Seth, S., Ahmed, T., De, A., Samanta, A.: Tackling the defects, stability, and photoluminescence of CsPbX3 perovskite nanocrystals. ACS Energy Lett. **4**(7), 1610–1618 (2019). https://doi.org/10.1021/ACSENERGYLETT.9B00849
189. Moon, B.J., et al.: Rare-earth-element-ytterbium-substituted lead-free inorganic perovskite nanocrystals for optoelectronic applications. Adv. Mater. **31**(33), 1901716 (2019). https://doi.org/10.1002/ADMA.201901716
190. Chen, Q., et al.: Under the spotlight: the organic–inorganic hybrid halide perovskite for optoelectronic applications. Nano Today **10**(3), 355–396 (2015). https://doi.org/10.1016/J.NANTOD.2015.04.009
191. La Porta, F.A., Masi, S.: Solvent-mediated structural evolution mechanism from Cs4PbBr 6 to CsPbBr3 crystals. Nanomanufacturing **1**(2), 67–74 (2021). https://doi.org/10.3390/nanomanufacturing1020007
192. Cheng, Y., Ding, L.: Pushing commercialization of perovskite solar cells by improving their intrinsic stability. Energy Environ. Sci. **14**(6), 3233–3255 (2021). https://doi.org/10.1039/D1EE00493J
193. Bibi, A., et al.: Lead-free halide double perovskites: toward stable and sustainable optoelectronic devices. Mater. Today **49**, 123–144 (2021). https://doi.org/10.1016/J.MATTOD.2020.11.026
194. Hao, J., Xiao, X.: Recent development of optoelectronic application based on metal halide perovskite nanocrystals. Front. Chem. **9**, 1130 (2022). https://doi.org/10.3389/FCHEM.2021.822106/BIBTEX
195. Hoefler, S.F., Trimmel, G., Rath, T.: Progress on lead-free metal halide perovskites for photovoltaic applications: a review. Monatshefte für Chemie—Chem. Mon. **148**(5), 795–826 (2017). https://doi.org/10.1007/s00706-017-1933-9
196. Sun, J., Yang, J., Lee, J.I., Cho, J.H., Kang, M.S.: Lead-free perovskite nanocrystals for light-emitting devices. J. Phys. Chem. Lett. **9**(7), 1573–1583 (2018). https://doi.org/10.1021/ACS.JPCLETT.8B00301
197. Manzhos, S., et al.: Materials design and optimization for next-generation solar cell and light-emitting technologies. J. Phys. Chem. Lett. **12**(19), 4638–4657 (2021). https://doi.org/10.1021/ACS.JPCLETT.1C00714
198. Jeong, S.H., et al.: Characterizing the efficiency of perovskite solar cells and light-emitting diodes. Joule **4**(6), 1206–1235 (2020). https://doi.org/10.1016/J.JOULE.2020.04.007
199. Wang, F., Liu, X.K., Gao, F.: Fundamentals of solar cells and light-emitting diodes. Adv. Nanomater. Sol. Cells Light Emit. Diodes 1–35 (2019). https://doi.org/10.1016/B978-0-12-813647-8.00001-1

200. Xu, L., Yuan, S., Zeng, H., Song, J.: A comprehensive review of doping in perovskite nanocrystals/quantum dots: evolution of structure, electronics, optics, and light-emitting diodes. Mater. Today Nano **6**, 100036 (2019). https://doi.org/10.1016/J.MTNANO.2019.100036
201. Van Le, Q., Won Jang, H., Young Kim, S., V Le, Q., Kim, S.Y., Jang, H.W.: Recent advances toward high-efficiency halide perovskite light-emitting diodes: review and perspective. Small Meth. **2**(10), 1700419 (2018). https://doi.org/10.1002/SMTD.201700419
202. Guner, T., Demir, M.M.: A review on halide perovskites as color conversion layers in white light emitting diode applications. Phys. Status Solidi **215**(13), 1800120 (2018). https://doi.org/10.1002/PSSA.201800120
203. Ji, K., et al.: Halide perovskite light-emitting diode technologies. Adv. Opt. Mater. **9**(18), 2002128 (2021). https://doi.org/10.1002/ADOM.202002128
204. Su, Y., et al.: Highly controllable and efficient synthesis of mixed-halide CsPbX3 (X = Cl, Br, I) perovskite QDs toward the tunability of entire visible light. ACS Appl. Mater. Interfaces **9**(38), 33020–33028 (2017). https://doi.org/10.1021/ACSAMI.7B10612/SUPPL_FILE/AM7B10612_SI_001.PDF
205. Eperon, G.E., Stranks, S.D., Menelaou, C., Johnston, M.B., Herz, L.M., Snaith, H.J.: Formamidinium lead trihalide: a broadly tunable perovskite for efficient planar heterojunction solar cells. Energy Environ. Sci. **7**(3), 982–988 (2014). https://doi.org/10.1039/C3EE43822H
206. Ng, Y.F., et al.: Highly efficient Cs-based perovskite light-emitting diodes enabled by energy funnelling. Chem. Commun. **53**(88), 12004–12007 (2017). https://doi.org/10.1039/C7CC06615E
207. Byun, J., et al.: Efficient visible quasi-2D perovskite light-emitting diodes. Adv. Mater. **28**(34), 7515–7520 (2016). https://doi.org/10.1002/ADMA.201601369
208. Tsai, H., et al.: Stable light-emitting diodes using phase-pure Ruddlesden-popper layered perovskites. Adv. Mater. **30**(6), 1704217 (2018). https://doi.org/10.1002/ADMA.201704217
209. El-Ballouli, A.O., Bakr, O.M., Mohammed, O.F.: Structurally tunable two-dimensional layered perovskites: from confinement and enhanced charge transport to prolonged hot carrier cooling dynamics. J. Phys. Chem. Lett. **11**(14), 5705–5718 (2020). https://doi.org/10.1021/ACS.JPCLETT.0C00359
210. Zhang, L., et al.: High-performance quasi-2D perovskite light-emitting diodes: from materials to devices. Light Sci. Appl. **10**(1), 1–26 (2021). https://doi.org/10.1038/s41377-021-00501-0
211. Yin, J., Li, H., Cortecchia, D., Soci, C., Brédas, J.L.: Excitonic and polaronic properties of 2D hybrid organic-inorganic perovskites. ACS Energy Lett. **2**(2), 417–423 (2017). https://doi.org/10.1021/ACSENERGYLETT.6B00659/SUPPL_FILE/NZ6B00659_SI_001.PDF
212. Kahmann, S., Tekelenburg, E.K., Duim, H., Kamminga, M.E., Loi, M.A.: Extrinsic nature of the broad photoluminescence in lead iodide-based Ruddlesden–Popper perovskites. Nat. Commun. **11**(1), 1–8 (2020). https://doi.org/10.1038/s41467-020-15970-x
213. Chen, Z., et al.: High-performance color-tunable perovskite light emitting devices through structural modulation from bulk to layered film. Adv. Mater. **29**(8), 1603157 (2017). https://doi.org/10.1002/ADMA.201603157
214. Yang, X., et al.: Efficient green light-emitting diodes based on quasi-two-dimensional composition and phase engineered perovskite with surface passivation. Nat. Commun. **9**(1), 1–8 (2018). https://doi.org/10.1038/s41467-018-02978-7
215. Quan, L.N., et al.: Tailoring the energy landscape in quasi-2D halide perovskites enables efficient green-light emission. Nano Lett. **17**(6), 3701–3709 (2017). https://doi.org/10.1021/ACS.NANOLETT.7B00976/SUPPL_FILE/NL7B00976_SI_001.PDF
216. Wei, Q., Ning, Z.: Emerging highly emissive and stable white emitting 'phosphores' based on lead-free inorganic halide perovskites. Sci. China Chem. **62**(3), 287–288 (2018). https://doi.org/10.1007/S11426-018-9391-8

217. Luo, J., et al.: Efficient and stable emission of warm-white light from lead-free halide double perovskites. Nature **563**(7732), 541–545 (2018). https://doi.org/10.1038/s41586-018-0691-0
218. de Holanda, M.S., Moral, R.F., Marchezi, P.E., Marques, F.C., Nogueira, A.F.: Layered metal halide perovskite solar cells: a review from structure-properties perspective towards maximization of their performance and stability. EcoMat **3**(4), e12124 (2021). https://doi.org/10.1002/EOM2.12124
219. Pal, J., et al.: Synthesis and optical properties of colloidal M3Bi2I9 (M = Cs, Rb) perovskite nanocrystals. J. Phys. Chem. C **122**(19), 10643–10649 (2018). https://doi.org/10.1021/ACS.JPCC.8B03542/SUPPL_FILE/JP8B03542_SI_001.PDF
220. Bass, K.K., et al.: Vibronic structure in room temperature photoluminescence of the halide perovskite Cs3Bi2Br 9. Inorg. Chem. **56**(1), 42–45 (2017). https://doi.org/10.1021/ACS.INORGCHEM.6B01571/SUPPL_FILE/IC6B01571_SI_001.PDF
221. Jun, T., et al.: Lead-free highly efficient blue-emitting Cs3Cu2I5 with 0D electronic structure. Adv. Mater. **30**(43), 1804547 (2018). https://doi.org/10.1002/ADMA.201804547
222. Ma, Z., et al.: Electrically-driven violet light-emitting devices based on highly stable lead-free perovskite Cs 3 Sb 2 Br 9 quantum dots. ACS Energy Lett. **5**(2), 385–394 (2020). https://doi.org/10.1021/acsenergylett.9b02096
223. Han, P., et al.: Size effect of lead-free halide double perovskite on luminescence property. Sci. China Chem. **62**(10), 1405–1413 (2019). https://doi.org/10.1007/s11426-019-9520-1
224. Zhou, C., et al.: Luminescent zero-dimensional organic metal halide hybrids with near-unity quantum efficiency. Chem. Sci. **9**(3), 586–593 (2018). https://doi.org/10.1039/C7SC04539E
225. Zhang, X., et al.: Bright orange electroluminescence from lead-free two-dimensional perovskites. ACS Energy Lett. **4**(1), 242–248 (2019). https://doi.org/10.1021/ACSENERGYLETT.8B02239/SUPPL_FILE/NZ8B02239_SI_001.PDF
226. Hong, W.L., et al.: Efficient low-temperature solution-processed lead-free perovskite infrared light-emitting diodes. Adv. Mater. **28**(36), 8029–8036 (2016). https://doi.org/10.1002/adma.201601024
227. Lai, M.L., et al.: Tunable near-infrared luminescence in tin halide perovskite devices. J. Phys. Chem. Lett. **7**(14), 2653–2658 (2016). https://doi.org/10.1021/acs.jpclett.6b01047
228. Liang, H., et al.: High color purity lead-free perovskite light-emitting diodes via Sn stabilization. Adv. Sci. **7**(8), 1903213 (2020). https://doi.org/10.1002/ADVS.201903213
229. Wang, Y., et al.: Tin-based multiple quantum well perovskites for light-emitting diodes with improved stability. J. Phys. Chem. Lett. **10**(3), 453–459 (2019). https://doi.org/10.1021/ACS.JPCLETT.8B03700/SUPPL_FILE/JZ8B03700_SI_001.PDF
230. Ma, Z., et al.: Stable yellow light-emitting devices based on ternary copper halides with broadband emissive self-trapped excitons. ACS Nano **14**(4), 4475–4486 (2020). https://doi.org/10.1021/ACSNANO.9B10148/SUPPL_FILE/NN9B10148_SI_001.PDF
231. Wang, L., et al.: Colloidal synthesis of ternary copper halide nanocrystals for high-efficiency deep-blue light-emitting diodes with a half-lifetime above 100 h. Nano Lett. **20**(5), 3568–3576 (2020). https://doi.org/10.1021/ACS.NANOLETT.0C00513/SUPPL_FILE/NL0C00513_SI_001.PDF
232. Ma, Z., et al.: Electrically-driven violet light-emitting devices based on highly stable lead-free perovskite Cs3Sb2Br 9 quantum dots. ACS Energy Lett. **5**, 385–394 (2019). https://doi.org/10.1021/acsenergylett.9b02096
233. Liu, Z., et al.: Anti-solvent spin-coating for improving morphology of lead-free (CH3NH3)3Bi2I9 perovskite films. SN Appl. Sci. **1**(7), 706 (2019). https://doi.org/10.1007/s42452-019-0727-6
234. Nguyen, B.P., et al.: Phase formation and local charge transport of lead-free CH3NH3Sn(I1−xBrx)3 ($0 \leq x \leq 1$) perovskite solar cells fabricated by solvent optimization. Sol. Energy **186**, 136–144 (2019). https://doi.org/10.1016/j.solener.2019.05.007

235. Park, B.-W., Philippe, B., Zhang, X., Rensmo, H., Boschloo, G., Johansson, E.M.J.: Bismuth based hybrid perovskites A 3 Bi 2 I 9 (A: methylammonium or cesium) for solar cell application. Adv. Mater. **27**(43), 6806–6813 (2015). https://doi.org/10.1002/adma.201501978
236. Ke, W., et al.: Efficient lead-free solar cells based on hollow {en}MASnI 3 perovskites. J. Am. Chem. Soc. **139**(41), 14800–14806 (2017). https://doi.org/10.1021/jacs.7b09018
237. Gupta, S., Bendikov, T., Hodes, G., Cahen, D.: CsSnBr 3, a lead-free halide perovskite for long-term solar cell application: insights on SnF 2 addition. ACS Energy Lett. **1**(5), 1028–1033 (2016). https://doi.org/10.1021/acsenergylett.6b00402
238. Hao, F., Stoumpos, C.C., Cao, D.H., Chang, R.P.H., Kanatzidis, M.G.: Lead-free solid-state organic–inorganic halide perovskite solar cells. Nat. Photonics **8**(6), 489–494 (2014). https://doi.org/10.1038/nphoton.2014.82
239. Nishikubo, R., et al.: Optoelectronic and energy level exploration of bismuth and antimony-based materials for lead-free solar cells. Chem. Mater. **32**(15), 6416–6424 (2020). https://doi.org/10.1021/acs.chemmater.0c01503
240. Zhang, X., et al.: Active-layer evolution and efficiency improvement of (CH3NH3 3Bi2I9-based solar cell on TiO2-deposited ITO substrate. Nano Res. **9**(10), 2921–2930 (2016). https://doi.org/10.1007/s12274-016-1177-8
241. Pantaler, M., et al.: Hysteresis-free lead-free double-perovskite solar cells by interface engineering. ACS Energy Lett. **3**(8), 1781–1786 (2018). https://doi.org/10.1021/acsenergylett.8b00871
242. Kumar, M.H., et al.: Lead-free halide perovskite solar cells with high photocurrents realized through vacancy modulation. Adv. Mater. **26**(41), 7122–7127 (2014). https://doi.org/10.1002/adma.201401991
243. Chen, L.-J., Lee, C.-R., Chuang, Y.-J., Wu, Z.-H., Chen, C.: Synthesis and optical properties of lead-free cesium tin halide perovskite quantum rods with high-performance solar cell application. J. Phys. Chem. Lett. **7**(24), 5028–5035 (2016). https://doi.org/10.1021/acs.jpclett.6b02344
244. Wu, C., et al.: The dawn of lead-free perovskite solar cell: highly stable double perovskite Cs 2 AgBiBr 6 film. Adv. Sci. **5**(3), 1700759 (2018). https://doi.org/10.1002/advs.201700759
245. Harikesh, P.C., et al.: Rb as an alternative cation for templating inorganic lead-free perovskites for solution processed photovoltaics. Chem. Mater. **28**(20), 7496–7504 (2016). https://doi.org/10.1021/acs.chemmater.6b03310
246. Zhu, Z., Chueh, C., Li, N., Mao, C., Jen, A.K.-Y.: Realizing efficient lead-free formamidinium tin triiodide perovskite solar cells via a sequential deposition route. Adv. Mater. **30**(6), 1703800 (2018). https://doi.org/10.1002/adma.201703800
247. Ning, W., et al.: Long electron-hole diffusion length in high-quality lead-free double perovskite films. Adv. Mater. **30**(20), 1706246 (2018). https://doi.org/10.1002/adma.201706246
248. Rahul, P.K., Singh, R., Singh, V., Singh, B., Bhattacharya, Khan, Z.H.: New class of lead free perovskite material for low-cost solar cell application. Mater. Res. Bull. **97**, 572–577 (2018). https://doi.org/10.1016/j.materresbull.2017.09.054
249. Gao, W., et al.: High-quality Cs 2 AgBiBr 6 Double perovskite film for lead-free inverted planar heterojunction solar cells with 2.2 % efficiency. ChemPhysChem **19**(14), 1696–1700 (2018). https://doi.org/10.1002/cphc.201800346
250. Baltakesmez, A., Güzeldir, B., Alkan, Y., Sağlam, M., Biber, M.: Optimizing quality of lead-free perovskite thin film with anti-solvent engineering and co-doping SnBr2/SnF2; its solar cell performance. Opt. Mater. (Amst). **110**, 110524 (2020). https://doi.org/10.1016/j.optmat.2020.110524
251. He, L., et al.: Efficient anti-solvent-free spin-coated and printed Sn-perovskite solar cells with crystal-based precursor solutions. Matter **2**(1), 167–180 (2020). https://doi.org/10.1016/j.matt.2019.10.006

252. Jokar, E., Cheng, P.-Y., Lin, C.-Y., Narra, S., Shahbazi, S., Wei-Guang Diau, E.: Enhanced performance and stability of 3D/2D tin perovskite solar cells fabricated with a sequential solution deposition. ACS Energy Lett. **6**(2), 485–492 (2021). https://doi.org/10.1021/acsenergylett.0c02305
253. Ng, C.H., et al.: Reducing trap density and carrier concentration by a Ge additive for an efficient quasi 2D/3D perovskite solar cell. J. Mater. Chem. A **8**(6), 2962–2968 (2020). https://doi.org/10.1039/C9TA11989B
254. Liu, J., et al.: Lead-free solar cells based on tin halide perovskite films with high coverage and improved aggregation. Angew. Chemie **130**(40), 13405–13409 (2018). https://doi.org/10.1002/ange.201808385
255. Chen, M., et al.: High-performance lead-free solar cells based on tin-halide perovskite thin films functionalized by a divalent organic cation. ACS Energy Lett. **5**(7), 2223–2230 (2020). https://doi.org/10.1021/acsenergylett.0c00888
256. Ran, C., et al.: Construction of compact methylammonium bismuth iodide film promoting lead-free inverted planar heterojunction organohalide solar cells with open-circuit voltage over 0.8 V. J. Phys. Chem. Lett. **8**(2), 394–400 (2017). https://doi.org/10.1021/acs.jpclett.6b02578
257. Boopathi, K.M., et al.: Solution-processable antimony-based light-absorbing materials beyond lead halide perovskites. J. Mater. Chem. A **5**(39), 20843–20850 (2017). https://doi.org/10.1039/C7TA06679A
258. Jokar, E., Chien, C.-H., Tsai, C.-M., Fathi, A., Diau, E.W.-G.: Robust tin-based perovskite solar cells with hybrid organic cations to attain efficiency approaching 10%. Adv. Mater. **31**(2), 1804835 (2019). https://doi.org/10.1002/adma.201804835
259. Vidal, R., et al.: Assessing health and environmental impacts of solvents for producing perovskite solar cells. Nat. Sustain. **4**(3), 277–285 (2020). https://doi.org/10.1038/s41893-020-00645-8
260. Correa-Baena, J.-P., et al.: A -site cation in inorganic A 3 Sb 2 I 9 perovskite influences structural dimensionality, exciton binding energy, and solar cell performance. Chem. Mater. **30**(11), 3734–3742 (2018). https://doi.org/10.1021/acs.chemmater.8b00676
261. Nie, R., Mehta, A., Park, B., Kwon, H.-W., Im, J., Il Seok, S.: Mixed sulfur and iodide-based lead-free perovskite solar cells. J. Am. Chem. Soc. **140**(3), 872–875 (2018). https://doi.org/10.1021/jacs.7b11332
262. Weiss, M., Horn, J., Richter, C., Schlettwein, D.: Preparation and characterization of methylammonium tin iodide layers as photovoltaic absorbers. Phys. Status Solidi **213**(4), 975–981 (2016). https://doi.org/10.1002/PSSA.201532594
263. Cortecchia, D., et al.: Lead-free MA2CuClxBr 4–x hybrid perovskites. Inorg. Chem. **55**(3), 1044–1052 (2016). https://doi.org/10.1021/ACS.INORGCHEM.5B01896/SUPPL_FILE/IC5B01896_SI_001.PDF
264. Abulikemu, M., et al.: Optoelectronic and photovoltaic properties of the air-stable organohalide semiconductor (CH3NH3)3Bi2I9. J. Mater. Chem. A **4**(32), 12504–12515 (2016). https://doi.org/10.1039/C6TA04657F
265. Greul, E., Petrus, M.L., Binek, A., Docampo, P., Bein, T.: Highly stable, phase pure Cs2AgBiBr 6 double perovskite thin films for optoelectronic applications. J. Mater. Chem. A **5**(37), 19972–19981 (2017). https://doi.org/10.1039/C7TA06816F
266. Wu, C., et al.: The dawn of lead-free perovskite solar cell: highly stable double perovskite Cs2AgBiBr 6 film. Adv. Sci. **5**(3), 1700759 (2018). https://doi.org/10.1002/ADVS.201700759
267. Li, P., Gao, W., Ran, C., Dong, H., Hou, X., Wu, Z.: Post-treatment engineering of vacuum-deposited Cs2NaBiI6 double perovskite film for enhanced photovoltaic performance. Phys. Status Solidi **216**(23), 1900567 (2019). https://doi.org/10.1002/PSSA.201900567
268. Ke, W., Kanatzidis, M.G.: Prospects for Low-Toxicity Lead-Free Perovskite Solar Cells, pp. 1–4 (2019)

269. Tiwari, A., Satpute, N.S., Mehare, C.M., Dhoble, S.J.: Challenges, recent advances and improvements for enhancing the efficiencies of ABX3-based PeLEDs (perovskites light emitting diodes): A review. J. Alloys Compd. **850**, 156827 (2021). https://doi.org/10.1016/J.JALLCOM.2020.156827
270. Jung, H.S., Park, N.G.: Perovskite solar cells: from materials to devices. Small **11**(1), 10–25 (2015). https://doi.org/10.1002/SMLL.201402767
271. Salhi, B., Wudil, Y.S., Hossain, M.K., Al-Ahmed, A., Al-Sulaiman, F.A.: Review of recent developments and persistent challenges in stability of perovskite solar cells. Renew. Sustain. Energy Rev. **90**, 210–222 (2018). https://doi.org/10.1016/J.RSER.2018.03.058
272. Fu, Q., et al.: Recent progress on the long-term stability of perovskite solar cells. Adv. Sci. **5**(5), 1700387 (2018). https://doi.org/10.1002/ADVS.201700387
273. Wang, Y., Sun, H.: Advances and prospects of lasers developed from colloidal semiconductor nanostructures. Prog. Quantum Electron. **60**, 1–29 (2018). https://doi.org/10.1016/J.PQUANTELEC.2018.05.002
274. Li, D., et al.: Recent progress on stability issues of organic-inorganic hybrid lead perovskite-based solar cells. RSC Adv. **6**, 89356–89366 (2016). https://doi.org/10.1039/c6ra19801e
275. He, S., Qiu, L., Ono, L.K., Qi, Y.: How far are we from attaining 10-year lifetime for metal halide perovskite solar cells? Mater. Sci. Eng. R Rep. **140**, 100545 (2020). https://doi.org/10.1016/J.MSER.2020.100545
276. Boyd, C.C., Cheacharoen, R., Leijtens, T., McGehee, M.D.: Understanding degradation mechanisms and improving stability of perovskite photovoltaics. Chem. Rev. **119**(5), 3418–3451 (2018). https://doi.org/10.1021/ACS.CHEMREV.8B00336
277. Khenkin, M.V., et al.: Consensus statement for stability assessment and reporting for perovskite photovoltaics based on ISOS procedures. Nat. Energy **5**(1), 35–49 (2020). https://doi.org/10.1038/s41560-019-0529-5
278. Anoop, K.M., et al.: Bias-dependent stability of perovskite solar cells studied using natural and concentrated sunlight. Sol. RRL **4**(2), 1900335 (2020). https://doi.org/10.1002/SOLR.201900335
279. Domanski, K., Alharbi, E.A., Hagfeldt, A., Grätzel, M., Tress, W.: Systematic investigation of the impact of operation conditions on the degradation behaviour of perovskite solar cells. Nat. Energy **3**(1), 61–67 (2018). https://doi.org/10.1038/s41560-017-0060-5
280. Saliba, M., Stolterfoht, M., Wolff, C.M., Neher, D., Abate, A.: Measuring aging stability of perovskite solar cells. Joule **2**(6), 1019–1024 (2018). https://doi.org/10.1016/J.JOULE.2018.05.005
281. Domanski, K., et al.: Migration of cations induces reversible performance losses over day/night cycling in perovskite solar cells. Energy Environ. Sci. **10**(2), 604–613 (2017). https://doi.org/10.1039/C6EE03352K
282. Christians, J.A., Manser, J.S., Kamat, P.V.: Best practices in perovskite solar cell efficiency measurements. Avoiding the error of making bad cells look good. J. Phys. Chem. Lett. **6**(5), 852–857 (2015). https://doi.org/10.1021/ACS.JPCLETT.5B00289
283. Yang, B., et al.: Outstanding passivation effect by a mixed-salt interlayer with internal interactions in perovskite solar cells. ACS Energy Lett. **5**(10), 3159–3167 (2020). https://doi.org/10.1021/ACSENERGYLETT.0C01664/SUPPL_FILE/NZ0C01664_SI_001.PDF
284. Heo, S., et al.: Origins of high performance and degradation in the mixed perovskite solar cells. Adv. Mater. **31**(8), 1805438 (2019). https://doi.org/10.1002/ADMA.201805438
285. Zhang, S., et al.: Barrier designs in perovskite solar cells for long-term stability. Adv. Energy Mater. **10**(35), 2001610 (2020). https://doi.org/10.1002/AENM.202001610
286. Hasan, O., Arif, A.F.M.: Performance and life prediction model for photovoltaic modules: effect of encapsulant constitutive behavior. Sol. Energy Mater. Sol. Cells **122**, 75–87 (2014). https://doi.org/10.1016/J.SOLMAT.2013.11.016
287. Wang, Y., et al.: Encapsulation and stability testing of perovskite solar cells for real life applications. ACS Mater. Au (2022). https://doi.org/10.1021/ACSMATERIALSAU.1C00045

288. Cheacharoen, R., Rolston, N., Harwood, D., Bush, K.A., Dauskardt, R.H., McGehee, M.D.: Design and understanding of encapsulated perovskite solar cells to withstand temperature cycling. Energy Environ. Sci. **11**(1), 144–150 (2018). https://doi.org/10.1039/C7EE02564E
289. Shi, L., et al.: Accelerated lifetime testing of organic-inorganic perovskite solar cells encapsulated by polyisobutylene. ACS Appl. Mater. Interfaces **9**(30), 25073–25081 (2017). https://doi.org/10.1021/ACSAMI.7B07625/SUPPL_FILE/AM7B07625_SI_001.PDF
290. Grancini, G., et al.: One-year stable perovskite solar cells by 2D/3D interface engineering. Nat. Commun. **8**(1), 1–8 (2017). https://doi.org/10.1038/ncomms15684
291. Stoichkov, V., Bristow, N., Troughton, J., De Rossi, F., Watson, T.M., Kettle, J.: Outdoor performance monitoring of perovskite solar cell mini-modules: diurnal performance, observance of reversible degradation and variation with climatic performance. Sol. Energy **170**, 549–556 (2018). https://doi.org/10.1016/J.SOLENER.2018.05.086
292. Hu, Y., et al.: Standardizing perovskite solar modules beyond cells. Joule **3**(9), 2076–2085 (2019). https://doi.org/10.1016/J.JOULE.2019.08.015
293. Velilla, E., Jaramillo, F., Mora-Seró, I.: High-throughput analysis of the ideality factor to evaluate the outdoor performance of perovskite solar minimodules. Nat. Energy **6**(1), 54–62 (2021). https://doi.org/10.1038/s41560-020-00747-9
294. Sharma, P., Kumar, S.: Bioremediation of heavy metals from industrial effluents by endophytes and their metabolic activity: recent advances. Bioresour. Technol. 125589 (2021)
295. Wang, J., et al.: Surface structure of mass-selected niobium oxide nanoclusters on Au(111) (2021). https://doi.org/10.1088/1361-6528/ac1cc0
296. Canil, L., et al.: Tuning halide perovskite energy levels. Energy Environ. Sci. **10**(3), 147–154 (2021). https://doi.org/10.1039/D0EE02216K
297. Alderete, B.L., et al.: Evaluation of toxicity and mutagenicity of a synthetic effluent containing azo dye after advanced oxidation process treatment. Chemosphere **263**, 128291 (2021)
298. Stroyuk, O.: Lead-free hybrid perovskites for photovoltaics. Beilstein J. Nanotechnol. **9**(1), 2209–2235 (2018). https://doi.org/10.3762/bjnano.9.207
299. Hao, F., Stoumpos, C.C., Chang, R.P.H., Kanatzidis, M.G.: Anomalous band gap behavior in mixed Sn and Pb perovskites enables broadening of absorption spectrum in solar cells. J. Am. Chem. Soc. **136**(22), 8094–8099 (2014). https://doi.org/10.1021/JA5033259/SUPPL_FILE/JA5033259_SI_001.PDF
300. Bin , T., et al.: Perovskite solar cells: film formation and properties. J. Mater. Chem. A **3**(17), 9032–9050 (2015). https://doi.org/10.1039/c4ta05246c
301. Hwang, K., et al.: Toward large scale roll-to-roll production of fully printed perovskite solar cells. Adv. Mater. **27**(7), 1241–1247 (2015). https://doi.org/10.1002/ADMA.201404598
302. Galagan, Y.: Perovskite solar cells: toward industrial-scale methods. J. Phys. Chem. Lett. **9**(15), 4326–4335 (2018). https://doi.org/10.1021/ACS.JPCLETT.8B01356
303. Qiu, L., He, S., Ono, L.K., Liu, S., Qi, Y.: Scalable fabrication of metal halide perovskite solar cells and modules. ACS Energy Lett. **4**(9), 2147–2167 (2019). https://doi.org/10.1021/ACSENERGYLETT.9B01396
304. Christians, J.A., et al.: Stability at scale: challenges of module interconnects for perovskite photovoltaics. ACS Energy Lett. **3**(10), 2502–2503 (2018). https://doi.org/10.1021/ACSENERGYLETT.8B01498/SUPPL_FILE/NZ8B01498_SI_001.PDF
305. Moon, S.J., et al.: Laser-scribing patterning for the production of organometallic halide perovskite solar modules. IEEE J. Photovoltaics **5**(4), 1087–1092 (2015). https://doi.org/10.1109/JPHOTOV.2015.2416913
306. Velilla Hernández, E.: Computational modeling of the electrical performance and degradation of third-generation photovoltaic modules, under accelerated and real operating conditions. Antioquia University (2021)
307. Booth, H.: Laser processing in industrial solar module manufacturing. JLMN-J. Laser Micro/Nanoeng. **5**(3) (2010). https://doi.org/10.2961/jlmn.2010.03.0001

308. Burn, A., et al.: All fiber laser scribing of Cu(In,Ga)Se2 thin-film solar modules. Phys. Proc. Complete(41), 713–722 (2013). https://doi.org/10.1016/J.PHPRO.2013.03.138
309. Green, M.A., et al.: Solar cell efficiency tables (version 49). Prog. Photovolt. Res. Appl. **25**(1), 3–13 (2017). https://doi.org/10.1002/PIP.2855
310. Green, M.A., Dunlop, E.D., Hohl-Ebinger, J., Yoshita, M., Kopidakis, N., Hao, X.: Solar cell efficiency tables (Version 58). Prog. Photovolt. Res. Appl. **29**(7), 657–667 (2021). https://doi.org/10.1002/PIP.3444
311. Odabaşı, Ç., Yıldırım, R.: Assessment of reproducibility, hysteresis, and stability relations in perovskite solar cells using machine learning. Energy Technol. **8**(12), 1901449 (2020). https://doi.org/10.1002/ENTE.201901449
312. Zhang, Z., et al.: High reproducibility of perovskite solar cells via a complete spin-coating sequential solution deposition process. Sol. Energy **122**, 97–103 (2015). https://doi.org/10.1016/J.SOLENER.2015.08.028
313. Petrović, M., Chellappan, V., Ramakrishna, S.: Perovskites: Solar cells & engineering applications—materials and device developments. Sol. Energy **122**, 678–699 (2015). https://doi.org/10.1016/J.SOLENER.2015.09.041
314. Green, M.A., Ho-Baillie, A., Snaith, H.J.: The emergence of perovskite solar cells. Nat. Photon. **8**(7), 506–514 (2014). Nature Publishing Group. https://doi.org/10.1038/nphoton.2014.134
315. Sun, W., et al.: Machine learning–assisted molecular design and efficiency prediction for high-performance organic photovoltaic materials. Sci. Adv. **5**(11) (2019. https://doi.org/10.1126/SCIADV.AAY4275/SUPPL_FILE/AAY4275_SM.PDF
316. Li, J., Pradhan, B., Gaur, S., Thomas, J.: Predictions and strategies learned from machine learning to develop high-performing perovskite solar cells. Adv. Energy Mater. **9**(46), 1901891 (2019). https://doi.org/10.1002/AENM.201901891